On the origin of the 100-kyr cycle in the astronomical forcing

André Berger, Marie-France Loutre, Jean-Luc Mélice

On the origin of the 100-kyr cycles in the astronomical forcing

A. Berger
Institut d'Astronomie et de Géophysique G. Lemaître, Université catholique de Louvain, Louvain-la-Neuve, Belgium

J. L. Mélice
Institut de Recherche pour le Développement/Department of Oceanography, University of Cape Town, Rondebosch, South Africa

M. F. Loutre
Institut d'Astronomie et de Géophysique G. Lemaître, Université catholique de Louvain, Louvain-la-Neuve, Belgium

Received 3 May 2005; revised 27 July 2005; accepted 8 September 2005; published 10 December 2005.

[1] Investigations during the last 25 years have demonstrated that the astronomically related 19-, 23-, and 41-kyr quasiperiodicities actually occur in long records of the Quaternary climate. However, the same investigations also identified the largest climatic cycle as being about 100 kyr long. As the 100-kyr variations in standing insolation due to eccentricity change are too small, they cannot be the direct cause of the ice ages. This is the reason why most of the modeling studies attempting to explain the relation between the astronomical forcing and climatic change have focused on this 100-kyr cycle. In this paper, we will show the astronomical origin of the periods at about 100 kyr that characterize the long-term variations of eccentricity, of its first derivative, of the frequency modulation of obliquity, and of the inclination of the Earth's orbit on the invariable plane of reference. Five independent values are found between 95 and 107 kyr, and a wavelet signature is suggested to test the possible relationships between the astronomical and climatic variables. Proxy records from deep-sea cores and European Programme for Ice Coring in Antarctica ice core and modeling results from the Louvain-la-Neuve two-dimensional model are used for illustration.

Citation: Berger, A., J. L. Mélice, and M. F. Loutre (2005), On the origin of the 100-kyr cycles in the astronomical forcing, *Paleoceanography*, *20*, PA4019, doi:10.1029/2005PA001173.

1. Astronomical Parameters

[2] The astronomical theory of paleoclimates [*Milankovitch*, 1941] holds that the long-term variations in the latitudinal and seasonal distributions of the solar energy received by the Earth are the causes of the great ice ages of the Pleistocene. Those variations are triggered by changes in three astronomical parameters [*A. Berger et al.*, 1993]: the eccentricity e, the obliquity ε, and the climatic precession $e \sin \tilde{\omega}$ ($\tilde{\omega}$ being the longitude of the perihelion measured from the moving equinox). Calculation of the planetary motion shows that the periods associated with the main terms in the Fourier expansion of these astronomical parameters [*Berger*, 1978] are close to 19 and 23 kyr for $e \sin \tilde{\omega}$, 41 kyr for ε and $\sim$100 and 400 kyr for e.

[3] In 1976, a paper by *Hays et al.* [1976] demonstrated from spectral analysis of climate sensitive indicators recorded in selected deep-sea cores that periods in the range of 100, 41, 23, and 19 kyr are significantly present over the last 500 kyr. Since then, spectral analysis of climatic records of the Quaternary [e.g., *Imbrie et al.*, 1992] and pre-Quaternary [e.g., *Shackleton et al.*, 1999] times provide substantial evidence that, at least near the frequencies of variation in obliquity and precession, a fraction of the climatic variance is driven by insolation changes. However, it is the variance components centered near 100 kyr which dominate most upper Pleistocene climatic records, more or less in phase with the eccentricity cycle [*Imbrie et al.*, 1993] or lagging it [*Shackleton*, 2000].

[4] It must be understood that not one of the time series discussed here, both the geological and the astronomical ones, is purely periodic. The claimed periods do not therefore characterize real cycles and are actually varying in time. Figure 1 shows clearly such instabilities in the so-called 100-kyr quasi-period both in the eccentricity [*Berger et al.*, 1998a] and the ODP806 oxygen isotopic record [*W. Berger et al.*, 1993] over the last 1.5 Myr. Let us stress that the amplitude of the 100-kyr oscillation in eccentricity decreases largely at approximately the time of the onset of the 100-kyr oscillation in the proxy climate sequence. Analyses of long deep-sea cores indicate indeed that both the amplitude and frequency of climatic variations have changed from 41 kyr to 100 kyr at about 900 kyr B.P. [*Pisias and Moore*, 1981; *Prell*, 1982; *Pestiaux and Berger*, 1984; *Ruddiman et al.*, 1986]. This observation and the weakening of the 100-kyr signal in eccentricity [*Berger et al.*, 1998a] provide an argument against any simple relationship between changes in eccentricity and in climate. This and the recognition that the amount of insolation perturbation at 100 kyr is much too small (less than 1% [*Berger*, 1977]) to cause a climate

0883-8305/05/2005PA001173

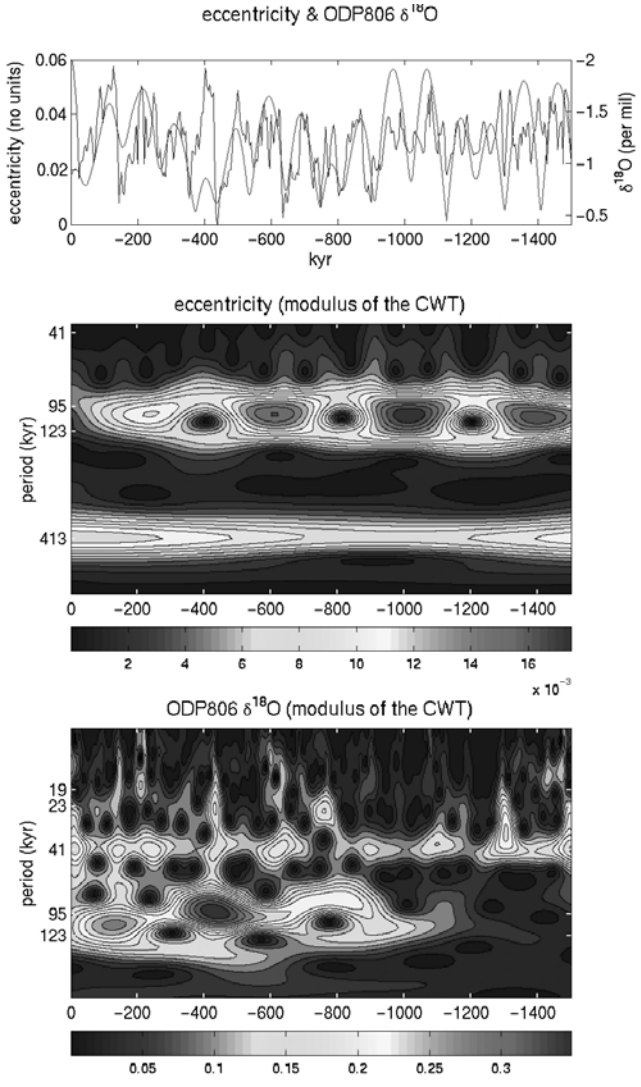

Figure 1. (top) Long-term variations and (middle and bottom) wavelet analysis of eccentricity [*Berger*, 1978] and $\delta^{18}O$ in Ocean Drilling Program (ODP) site 806 [*W. Berger et al.*, 1993]. See color version of this figure at back of this issue.

change of ice age amplitude explain why most modeling studies [e.g., *Claussen and Berger*, 2005; *Berger and Loutre*, 2005] have focused on the origin of the 100-kyr oscillations found in proxy climate records.

[5] Among others, a few papers attempted to relate the ~100-kyr period directly to one of the astronomical parameters. *Wigley* [1976] suggested a nonlinear response to precession (beating the two main frequencies of $e \sin \tilde{\omega}$: (1/19−1/23) equals ~ 1/100). *Rial* [1995] related the sawtooth shape of late Pleistocene paleoclimate records to the first derivative of e. *Liu* [1992] included the frequency variations of ε, and *Muller and MacDonald* [1995] claimed that the inclination of the Earth's orbital plane on the invariable plane, i', would remove some of the unresolved problems related to the "eccentricity" cycles found in geological records.

[6] It is out of the scope of this paper to review critically all these theories on the response of the climate system to these astronomical forcings (see, e.g., *Ridgwell et al.* [1999] for i'). We will focus first on the origin of the 100-kyr cycles found in these astronomical parameters, and second we will show how these parameters relate to the 100-kyr signal of a few proxy records. For the long-term variations of the astronomical parameters, both analytical [*Berger*, 1978; *Berger and Loutre*, 1991] and numerical [*Laskar et al.*, 1993; *Quinn et al.*, 1991] solutions exist. The analytical solution has the advantage of providing directly the frequencies, phases, and amplitudes of all terms of the trigonometrical expansion, but its accuracy is limited over roughly 1.5 Myr [*Berger and Loutre*, 1992]. As this is the time interval over which the most accurate proxy climate records exist, the solution by *Berger* [1978] will be used.

[7] The classical trigonometrical expansion used to compute the long-term behavior of e, ε, and $e \sin \tilde{\omega}$ is given by

$$e = e^* + \Sigma E_i \cos(\lambda_i t + \phi_i) \tag{1}$$

$$e \sin \tilde{\omega} = \Sigma P_i \sin(\alpha_i t + \eta_i) \tag{2}$$

$$\varepsilon = \varepsilon^* + \Sigma A_i \cos(\gamma_i t + \varsigma_i) \tag{3}$$

The amplitudes (E_i, P_i and A_i), the frequencies (λ_i, α_i and γ_i), and the phases are given by *Berger* [1978].

[8] Actually, equations (1), (2), and (3) originate from two systems of equations describing the long-term behavior of four fundamental astronomical parameters: e, π on the one hand and i, Ω on the other hand [e.g., *Bretagnon*, 1974].

[9] The long-term behavior of these parameters is given by

$$\begin{aligned} h &= e \sin \pi = \Sigma M_i \sin(g_i t + \beta_i) \\ k &= e \cos \pi = \Sigma M_i \cos(g_i t + \beta_i) \end{aligned} \tag{4}$$

$$\begin{aligned} p &= \sin i \sin \Omega = \Sigma N_i \sin(s_i t + \delta_i) \\ q &= \sin i \cos \Omega = \Sigma N_i \cos(s_i t + \delta_i) \end{aligned} \tag{5}$$

π is the longitude of the perihelion measured relatively to the fixed vernal equinox and is given by $\Omega + \omega$, Ω being the longitude of the ascending node and ω the argument of the perihelion. Here i is the inclination of the Earth's orbit (ecliptic) on a reference plane. Finally, $\tilde{\omega} = \pi + \psi$, where ψ, the general precession in longitude, is given by

$$\psi = kt + \alpha + \Sigma S_i \sin(\xi_i t + O_i) \tag{6}$$

k being the precessional constant. For the *Berger* [1978] solution, the work of *Bretagnon* [1974] was used for

Table 1. Most Important Terms in the Fourier Expansion of $e \sin \pi$, $e \sin \tilde{\omega}$, e, and de/dt Based Upon *Bretagnon* [1974] and *Berger* [1978][a]

Planet	Planet Number	Amplitude	Frequency, arc seconds/year	Phase, deg	Period, years
		$e \sin \pi$ [*Bretagnon*, 1974]			
J	5	0.018608	4.207	28.6	308,043
V	2	0.016275	7.346	193.8	176,420
M	4	−0.013007	17.857	308.3	72,576
E	3	0.009888	17.221	320.2	75,259
		$e \sin \tilde{\omega}$			
J	5	0.018608	54.646	32.0	23,716
V	2	0.016275	57.785	197.2	22,428
M	4	−0.013007	68.297	311.7	18,976
E	3	0.009888	67.660	323.6	19,155
		e			
V − J	2 − 5	0.011029	3.139	165.2	412,885
M − J	4 − 5	−0.008733	13.650	279.7	94,945
M − V	4 − 2	−0.007493	10.511	114.5	123,297
E − J	3 − 5	0.006724	13.013	291.6	99,590
E − V	3 − 2	0.005813	9.874	126.4	131,248
M − E	4 − 3	−0.004701	0.637	348.1	2,035,441
		de/dt			
	2 − 5	−0.16820[b]	3.139	165.2	412,885
	4 − 5	0.57773	13.650	279.7	94,945
	4 − 2	0.38212	10.511	114.5	123,297
	3 − 5	−0.42140	13.013	291.6	99,590
	3 − 2	−0.27610	9.874	126.4	131,248
	4 − 3	0.14722	0.637	348.1	2,035,441

[a]Planets involved are Venus (V), Earth (E), Mars (M), and Jupiter (J).
[b]These amplitudes for a change per kyr are multiplied by 10^3.

equations (4) and (5). Using the solutions by *Laskar* [1988] for equations (4) and (5) and *Berger and Loutre* [1991] for equation (1) to equation (3) gives only slightly different values for the periods involved and therefore would not change at all our line of argument.

2. Eccentricity

[10] The value of e can easily be numerically computed from

$$e = \sqrt{(e \sin \pi)^2 + (e \cos \pi)^2} \tag{7}$$

using equation (4), but it can also be obtained through a similar formula based upon the climatic precession, $e \sin \tilde{\omega}$ (equation (2)) instead of $e \sin \pi$ (equation (4)):

$$e \begin{matrix} \sin \\ \cos \end{matrix} \tilde{\omega} = \sum_{j=1}^{19} M_j \begin{matrix} \sin \\ \cos \end{matrix} \left((g_j + k)t + \beta_i + \alpha \right) + \Theta \tag{8}$$

where in the work of *Berger* [1978] Θ represents a long series of 570 higher-order terms, $k = 50.439273''$/year, and α is a constant equal to 3.393°. The most important terms are given in Table 1. In Table 1, each term is associated with a specific planet in agreement with sensitivity analysis performed in particular by *Bretagnon* [1974] in the calculation of the planetary motion. For example, the term with the largest amplitude for $e \sin \pi$ has a period of 308,043 years associated with g_5 and related to Jupiter (planet number 5). It leads to the largest amplitude term of $e \sin \tilde{\omega}$ with a period g_5' equal to 23,716 years ($g_5' = g_5 + k$).

[11] An analytical formula can also be developed [*Berger*, 1978] using equations (4) and (7):

$$e = e_0 + \sum_{k=1}^{171} b_k \cos \left(\gamma_k + \Theta \right) \tag{9}$$

where

$$e_0 = 0.0287$$

$$\sum b_k \cos \gamma_k = \sum_{i=1}^{18} \sum_{j=i+1}^{19} \frac{M_i M_j}{m} \cos \left[(g_i - g_j)t + (\beta_i - \beta_j) \right]$$

$$m = \sqrt{\sum_{i=1}^{19} M_i^2}$$

Θ represents the terms of higher order. From the most important terms of equation (9) given in Table 1, it is clear

that the so-called 400-kyr period comes from the combination tone $g_2 - g_5$ which involves mainly Venus and Jupiter and the two periods very close to 100 kyr ($b_2 = 94{,}945$ years and $b_4 = 99{,}590$ years) come respectively from $g_4 - g_5$ and $g_3 - g_5$, involving Mars and Jupiter and Earth and Jupiter.

[12] This shows also that the 123,297-year period is not only a combination tone of the frequencies associated with Mars and Venus but can also be generated as a combination tone of terms 1 and 2 of the eccentricity expansion itself; the same holds for 131,248 which can be generated by terms 1 and 4 of the eccentricity expansion. This leads us to conclude that among these five terms only three are independent, for example, b_1 equal to ~400 kyr and b_2 and b_4 equal to ~100 kyr.

[13] Similarly, using equations (7) and (8) leads, of course, to the same analytical development for e. However, the implication in terms of combination tones is more attractive as it links the eccentricity expansion to the climatic precession one and vice versa. In other words, we have $b_1 = g_2' - g_5'$, $b_2 = g_4' - g_5'$ and $b_4 = g_3' - g_5'$, with $g_i' = g_i + k$.

[14] This is the most straightforward demonstration that the 100-kyr and 400-kyr periods in eccentricity are already combination tones of the most important terms of precession: 412,885 comes strictly from 22,428 and 23,716, 94,945 comes from 18,976 and 23,716 and 99,590 comes from 19,155 and 23,716.

3. Derivative of Eccentricity

[15] One of the problems that the paleoclimatologists were facing analyzing the proxy record of the last million years is that they found most of the time a 100-kyr cycle [*Imbrie et al.*, 1993] with almost no or very little power centered on 400 kyr. Modeling the climate response to the astronomical forcing generates, on the contrary, a 400-kyr period as well as a 100-kyr one. However, since the late 1990s, this 400-kyr cycle appears to be more evident in proxy records, mainly from the Mesozoic [*Olsen and Kent*, 1999] but also from older geological periods (see *Shackleton et al.* [1999] and *Berger* [1989] for a review). The fact that there are unambiguous paleoclimatic data showing a clear 400-kyr periodicity points to eccentricity and/or its derivative as a direct or indirect cause of long-term climatic variations and not to the other astronomical variables, because this period is not present in i' (section 4) nor in the frequency modulation of ε (section 5). For the more recent periods, this 400 kyr looks, according to some data (e.g., the Indian Ocean coarse fraction of *Bassinot et al.* [1994]), closer to 500 kyr than to 400 kyr (Wang Pinxian, personal communication, 2003). It is expected that more reliable proxy record will us allow to solve this problem in the years to come.

[16] In the mean time, it is possible to generate an astronomical parameter which most important primary terms have a ~100-kyr period. This is the derivative of the eccentricity obtained directly from equation (1):

$$\frac{de}{dt} = -\sum E_i \lambda_i \sin(\lambda_i t + \phi_i) \qquad (10)$$

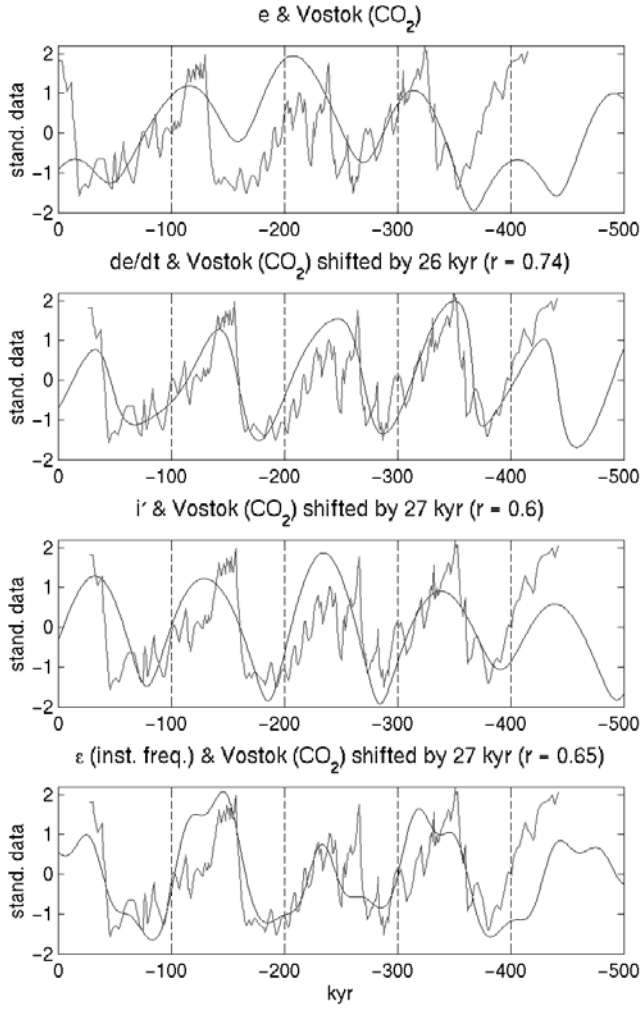

Figure 2. Long-term variations over the last 400 kyr of Vostok CO_2 concentration [*Petit et al.*, 1999], eccentricity, its first derivative, the inclination of the ecliptic on the invariable plane, and the frequency modulation of obliquity using the work of *Berger* [1978]. The time series of the last three parameters have been shifted forward by 26 and 27 kyr. See color version of this figure at back of this issue.

The frequencies in equation (10) are actually those existing in the expansion of e, but the amplitude associated with each term is multiplied by the frequency itself. As the ratio between the amplitudes associated with the 400-kyr and the 100-kyr cycles in equation (9) is less than the ratio between the periods themselves, the largest amplitude terms of de/dt are now associated with 100 kyr.

[17] The most important terms of equation (10) are listed in Table 1 from which it becomes evident that all 100-kyr terms are considerably reinforced as compared to equation (9), with an amplitude now of 2 to 4 times the amplitude of the 400-kyr term. This last becomes number 5 in decreasing order of the amplitudes and the two largest amplitude terms are definitely associated with the periods which are the closest to 100 kyr and related to M-J and

Table 2. Most Important Terms in the Expansion of i and i' Based Upon the Solution of *Bretagnon* [1974]

Planet	Planet Number	Amplitude	Frequency, arc seconds/year	Phase	Periods, years
		sin i sin Ω			
J	5	0.027672	0	106.1	-
E	3	0.020040	−18.8293	248.5	68,829
Me	1	0.012076	−5.6109	12.0	230,977
M	4	0.007609	−17.8188	277.4	72,732
V	2	0.005083	−6.7710	305.0	191,404
		sin i			
E − J	3 − 5	0.0005	−18.8293	142.4	68,829
Me − J	1 − 5	0.000334	−5.6109	265.9	230,977
M − J	4 − 5	0.000211	−17.8188	171.3	72,732
V − J	2 − 5	0.000141	−6.7710	198.9	191,404
		sin i'			
E − Me	3 − 1	0.000242	−13.2184	236.5	98,046
E − M	3 − 4	0.000152	−1.0105	331.1	1,282,533
E − V	3 − 2	0.000102	−12.0583	303.5	107,478
M − Me	4 − 1	0.000092	−12.2079	265.4	106,160
V − Me	2 − 1	0.000061	−1.1601	293.0	1,117,645
M − V	4 − 2	0.000039	−11.0478	332.4	117,308

E-J. Finally, as noted by *Rial* [1995], the *de*/*dt* curve (Figure 2) has a sawtooth shape accentuating the asymmetrical behavior of the eccentricity [*Berger et al.*, 1998a].

4. Inclination of the Earth's Orbital Plane

[18] One of the astronomical parameters intervening in the calculation of precession and obliquity is the inclination, i, of the Earth's orbital plane on the ecliptic of 1950.0 generally taken as the reference. Such angle is given by equation (5). The amplitudes, frequencies and phases are from *Bretagnon* [1974], and the most important terms are given in Table 2.

[19] Because of the importance of the mass of Jupiter in the mutual attraction of the planets and the Sun, the frequency associated with Jupiter (s_5) is equal to zero [*Bretagnon*, 1974]. The term corresponding to Jupiter is therefore a constant, and we have

$$\sin\ i \begin{matrix}\sin\\ \cos\end{matrix} \Omega = N_5 \begin{matrix}\sin\\ \cos\end{matrix} \delta_5 + \sum_{\substack{i=1\\ i\neq 5}}^{15} N_i \begin{matrix}\sin\\ \cos\end{matrix} (s_i t + \delta_i) \qquad (11)$$

If the reference plane is the invariable plane (the plane perpendicular to the axis of total angular momentum), the inclination i' is given by

$$\sin i' \begin{matrix}\sin\\ \cos\end{matrix} \Omega' = \sum_{\substack{i=1\\ i\neq 5}}^{15} N_i \begin{matrix}\sin\\ \cos\end{matrix} (s_i t + \delta_i) \qquad (12)$$

If the same technique developed to obtain the Fourier expansion of e (equation (9)) is used to compute i, we obtain

$$\sin i = C + \sum C_k \cos \zeta_k + \Theta \qquad (13)$$

where

$$\sum C_k \cos \zeta_k = \sum_{i=1}^{14} \sum_{j=i+1}^{15} \frac{N_i N_j}{n} \cos\left[(s_i - s_j)t + (\delta_i - \delta_j)\right]$$

Θ represents terms of higher order, C is a constant, and

$$n = \sqrt{\sum N_i^2}$$

As the amplitude associated with Jupiter is the largest, the largest terms for i in equation (13) come from the products involving N_5. However, as s_5 is equal to zero, the periods associated with these terms are those of sin i sin Ω and associated respectively to Earth, Mercury, Mars, and Venus. Therefore the spectrum of i is dominated by four periods, two of about 70 kyr (∼69 and 73 kyr) and two of about 210 kyr (∼231 and 191 kyr).

[20] If i' is now considered, the term number 5 is excluded, and the largest amplitudes are those coming from the Earth associated with Mercury, Mars, and Venus. In this case, the periods of the most important terms are given by $s_3 - s_1$ leading to 98,046 years and $s_3 - s_2$ leading to 107,478 years ($s_3 - s_4$ leads to a period of 1,282,533 years corresponding to the second most important term in amplitude as clearly seen in Figure 3c). Combination tones of s_4 with s_1 and s_2 lead also to periods not far from 100 kyr, 106,160 years and 117,308 years, but with a much lower amplitude.

[21] Consequently, as it is the case for eccentricity, periods close to 100 kyr appear but are certainly not identical to those appearing in the development of e. Moreover, there is no equivalent to climatic precession associated with this (i, Ω) system, as it was the case for the eccentricity. Therefore the 100-kyr periods in i' cannot be generated by a beat between two frequencies as it is for e;

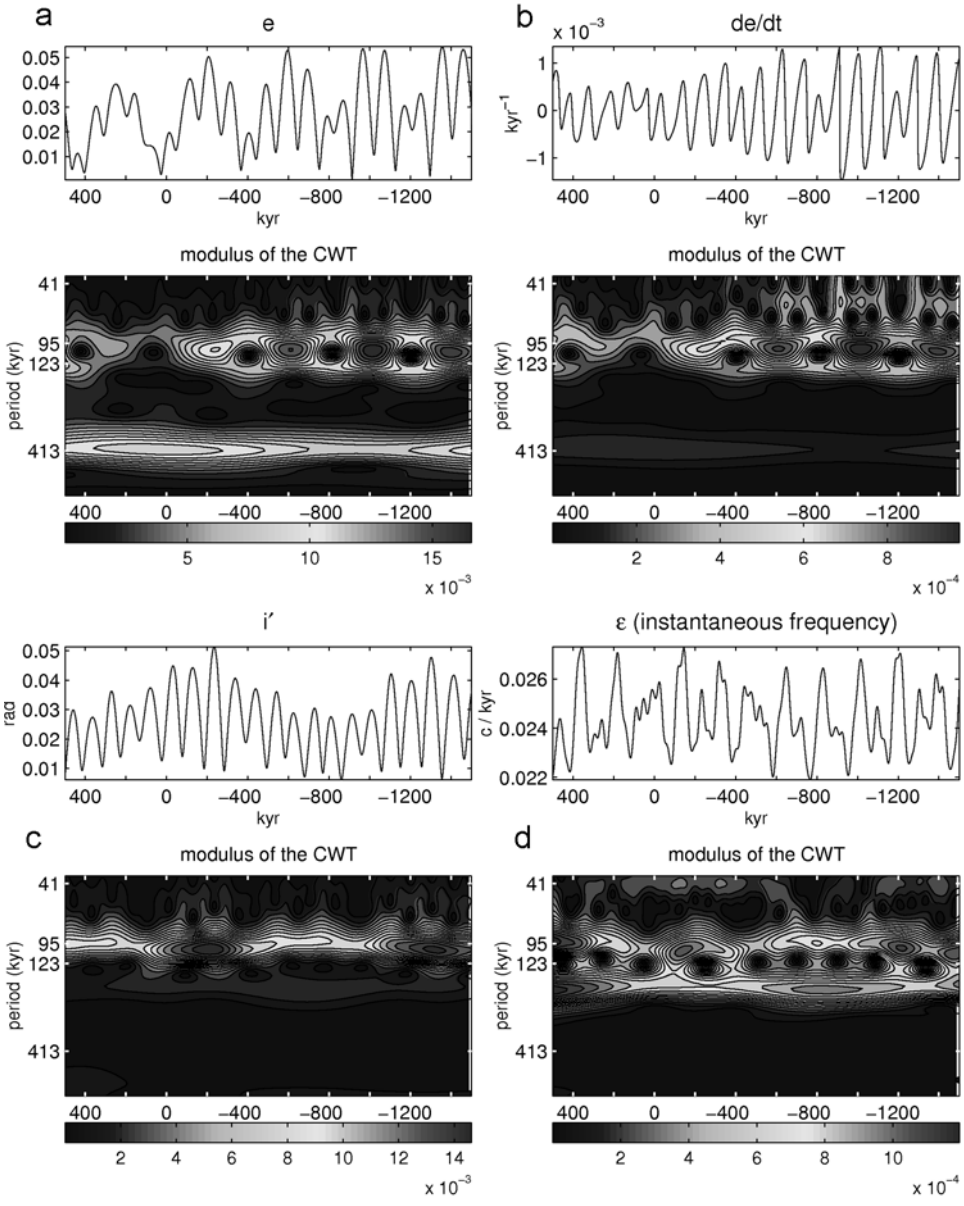

Figure 3. Wavelet analysis of (a) e, (b) de/dt, (c) i' and (d) the instantaneous frequency of ε from 1.5 Myr B.P. to 0.5 Myr A.P. (side effects have been eliminated using a much longer interval for the calculation). See color version of this figure at back of this issue.

they come only directly from the expansion of i' involving periods of about 70 kyr and 210 kyr.

5. Frequency Modulation of Obliquity

[22] The obliquity, ε, can be calculated from equation (3) where $\varepsilon^* = 23.321^\circ$ for *Berger* [1978]. The frequencies of the five largest amplitude terms are actually given by $s_3 + k$ (41 kyr), $s_4 + k$ (39,730 years), $s_6 + k$ (53,615 years), $s_{14} + k$ (40,521 years), and $s_1 + k$ (28,910 years), the most important one being definitely associated with 41 kyr. No one s_i frequency is sufficiently large, in absolute value, to lead to a 100-kyr cycle when combined with k. However, terms in $s_i - s_j$ occur also in the expansion of ε leading in particular to periods of 98,046 years and of 107,478 years. These are exactly those pointed out in i', but their associated amplitudes in the expansion of ε are much smaller (6.49″ and 3.4″, respectively, to be compared with the largest amplitude which is 2462.2″ in the expansion of ε).

[23] As a consequence, although the 41-kyr term dominates the expansion of ε, there is a variability around this period which is generated by the other terms and which leads to an amplitude and a frequency modulation. For the last million years, the spectra of these modulations display significant power at 171 and 97 kyr [*Mélice et al.*, 2001]. Again, a ~100-kyr period appears which is distinct from

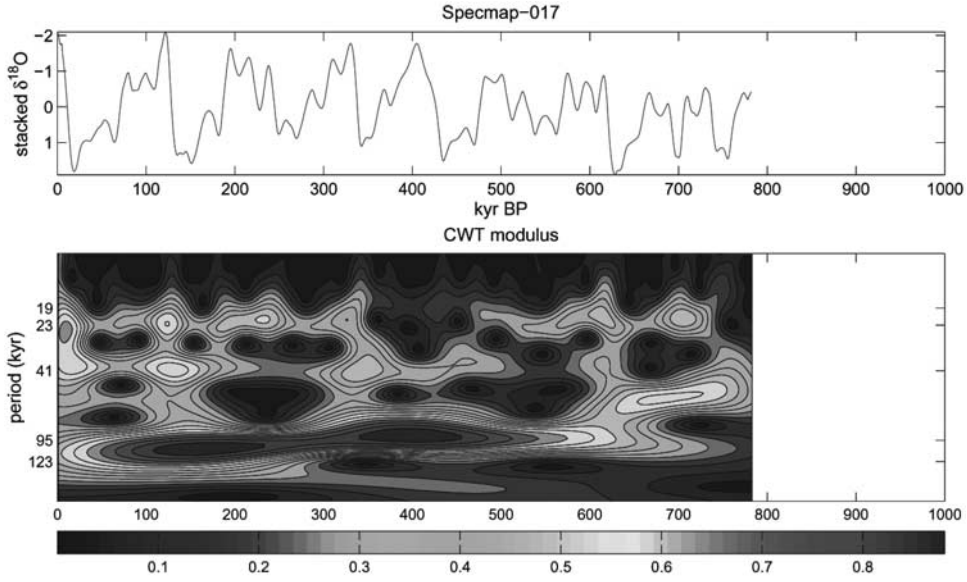

Figure 4. Long-term variations over the last 1 Myr of $\delta^{18}O$ for the (top) spectral mapping (SPECMAP) core and (bottom) a wavelet spectrum. See text for more explanation and references. See color version of this figure at back of this issue.

those characterizing e and i'. However, here this period explain less than 10% of the total variance of obliquity. This is largely different from e, de/dt, and i' where the 100-kyr components explain a much larger part of the total variance.

6. The 100-kyr Cycles in the Astronomical Parameters and in Proxy Records

[24] In order to illustrate the correlation between the astronomical parameters and proxy climate records, Figure 2 compares the Vostok CO_2 concentration over the last 400 kyr [*Petit et al.*, 1999] to the long-term variations of e, de/dt, and i' and the frequency modulation of ε. This record was chosen because of its quite accurate absolute chronology and is supposed to be a good standard target for Quaternary climate. The oxygen 18 values could have been chosen as in Figures 4–9, and it is expected that even better records will be made available soon [e.g., *EPICA Community Members*, 2004].

[25] In Figure 2, it can be seen that e compares relatively well with CO_2, especially for the phase as was already noted by *Hays et al.* [1976] from their $\delta^{18}O$ records (high

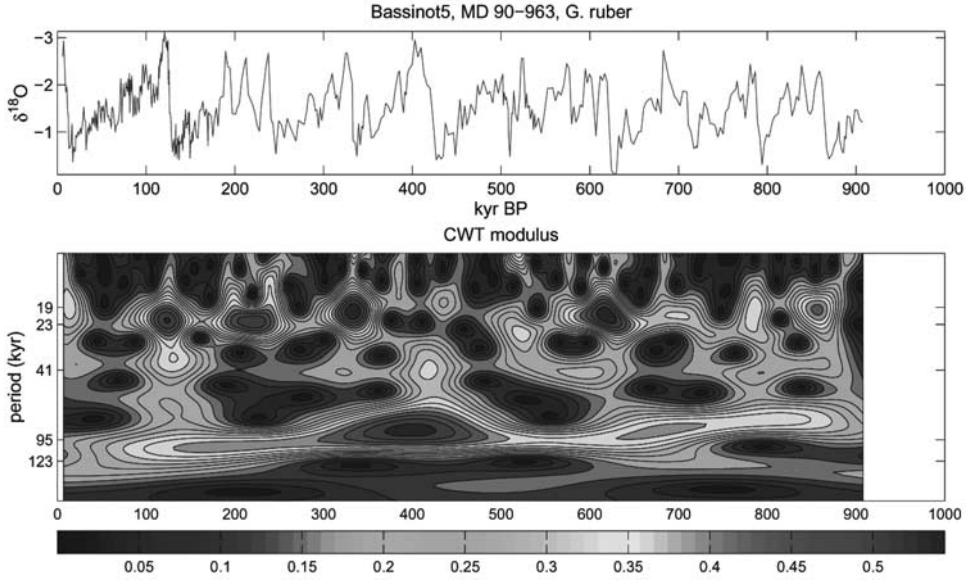

Figure 5. Same as Figure 4 but for the Bassinot core. See color version of this figure at back of this issue.

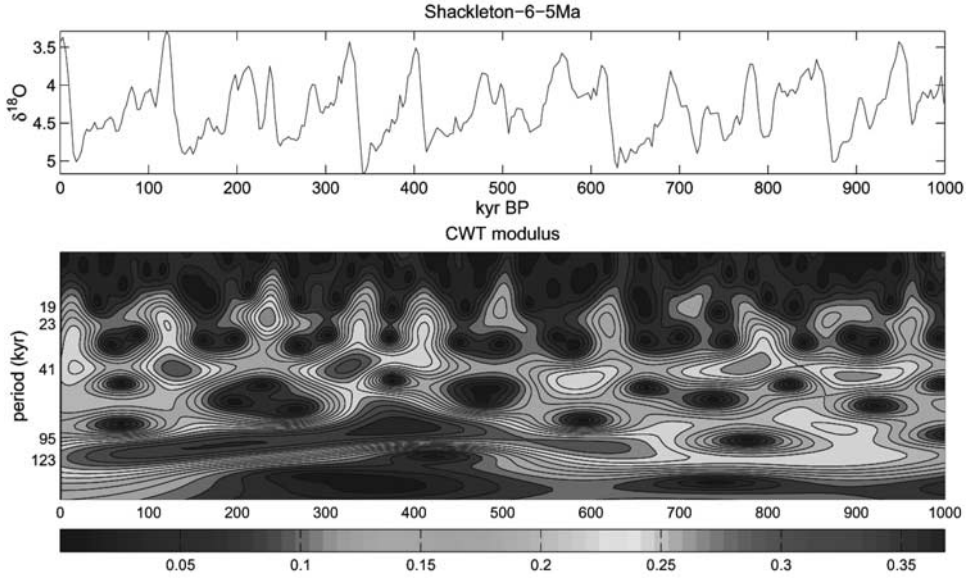

Figure 6. Same as Figure 4 but for the Shackleton core. See color version of this figure at back of this issue.

eccentricity at low ice volume). However, the low amplitude of e at stages 11 and 1 confirms the stage 11 problem already raised by *Imbrie et al.* [1993] and discussed in particular by *Berger and Loutre* [2003]. The amplitudes of the three other astronomical parameters are much more coherent with Vostok CO_2 than the amplitude of e. Analysis of the phase shows that they lead CO_2 by 26 kyr almost systematically, a shift forward by 26 or 27 kyr giving a correlation coefficient of 0.6 to 0.7 with CO_2.

[26] Such a comparison can also be made in the frequency domain. A wavelet analysis of the astronomical parameters is shown in Figure 3 for a period extending from 1.5 Myr B.P. to 0.5 Myr A.P. Figure 3 allows a straightforward comparison of the spectral properties of e, de/dt, and i' and the frequency modulation of ε from 1.5 Myr B.P. to 500 kyr A.P. The main differences between them relate (1) to the absence of a significant power at about 400 kyr except in e and (2) to a much narrower band localized around 98 kyr for i'; e, de/dt, and the instantaneous frequency of ε all show a larger number of periods in the 100-kyr period band. Such spectral structures are suggested to be used in addition to the time series (Figure 2) when discussing any possible

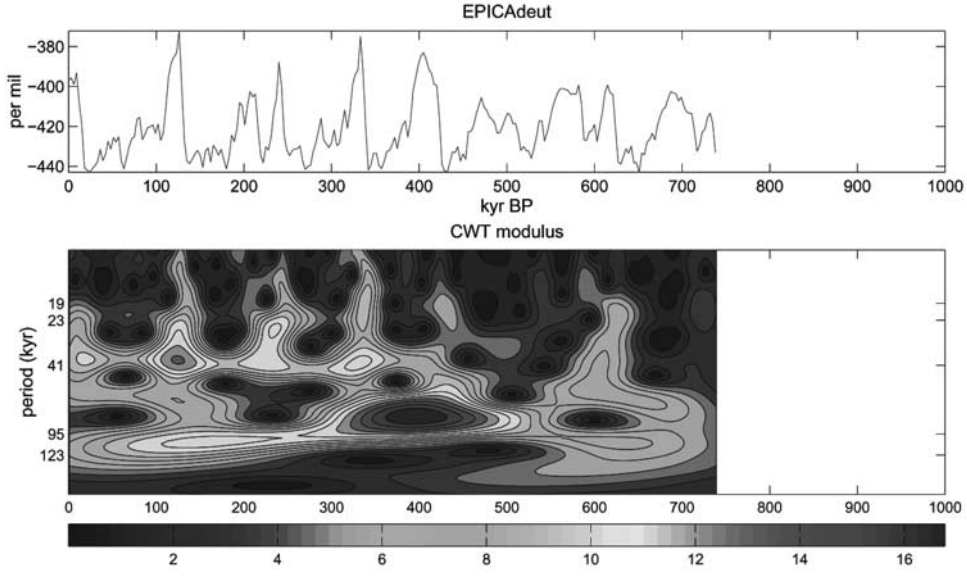

Figure 7. Same as Figure 4 but for the European Programme for Ice Coring in Antarctica (EPICA) deuterium core. See color version of this figure at back of this issue.

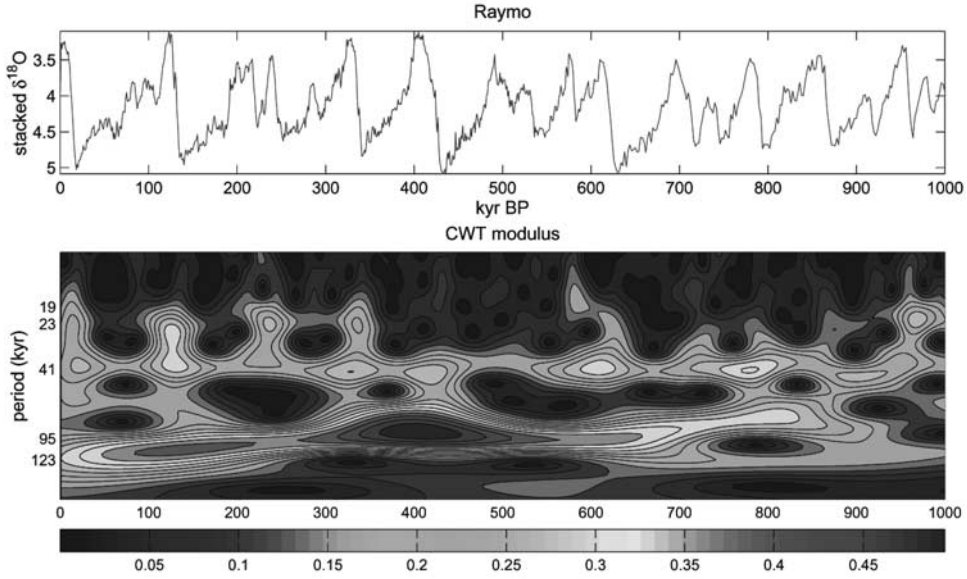

Figure 8. Same as Figure 4 but for the Lisiecki-Raymo core. See color version of this figure at back of this issue.

relationship between the astronomical parameters and proxy records. The following proxy records have been used: spectral mapping (SPECMAP) [*Imbrie et al.*, 1984; *Martinson et al.*, 1987] and those of *Bassinot et al.* [1994], *Shackleton and Pisias* [1985], *Shackleton et al.* [1990], *EPICA Community Members* [2004], *Lisiecki and Raymo* [2005], and *Tiedemann et al.* [1994]. The age models of all these data were tuned to the astronomical solution, and the age uncertainty is discussed in each reference. The data from Bassinot are from core MD90-0963 but with a higher resolution than published in 1994. The data from N. J. Shackleton and coworkers are a composite of records from cores V19-30 (top to 340 kyr B.P. [*Shackleton and Pisias*, 1985]) and ODP677 (340–1811 kyr B.P. [*Shackleton et al.*, 1990]). The data by Lisiecki and Raymo are a LR04 stack of benthic $\delta^{18}O$ records from 57 globally distributed sites tuned to a simple ice model based on 21 June insolation at 65°N. Tiedemann data are from Site 659. For SPECMAP and EPICA the data extend to 800 and 730 kyr B.P., respectively. For the other cores, only the last 1 Myr is used for which the chronology is assumed to be quite reasonable. In any case, it is not the purpose of this paper to critically discuss the absolute chronology of the different cores but rather to compare them

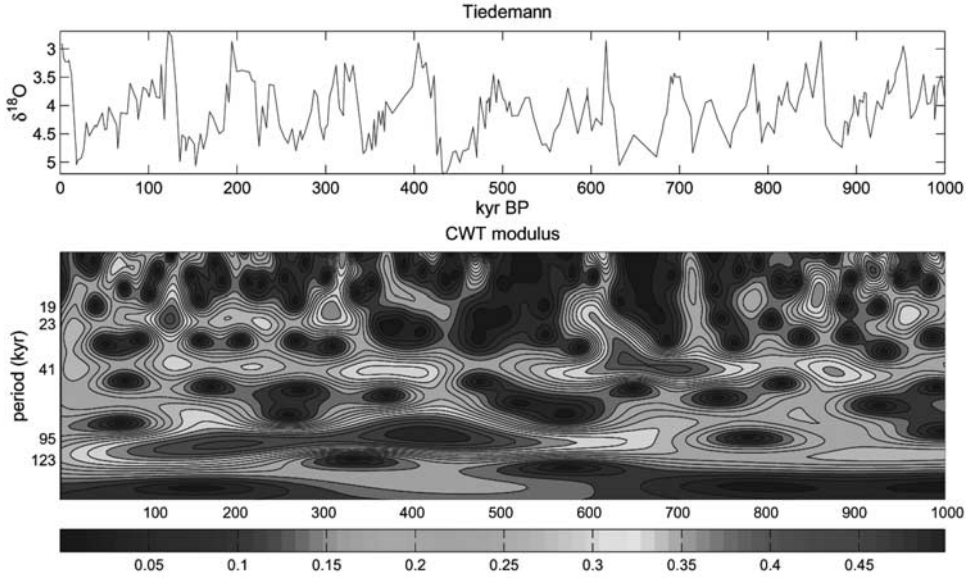

Figure 9. Same as Figure 4 but for the Tiedemann core. See color version of this figure at back of this issue.

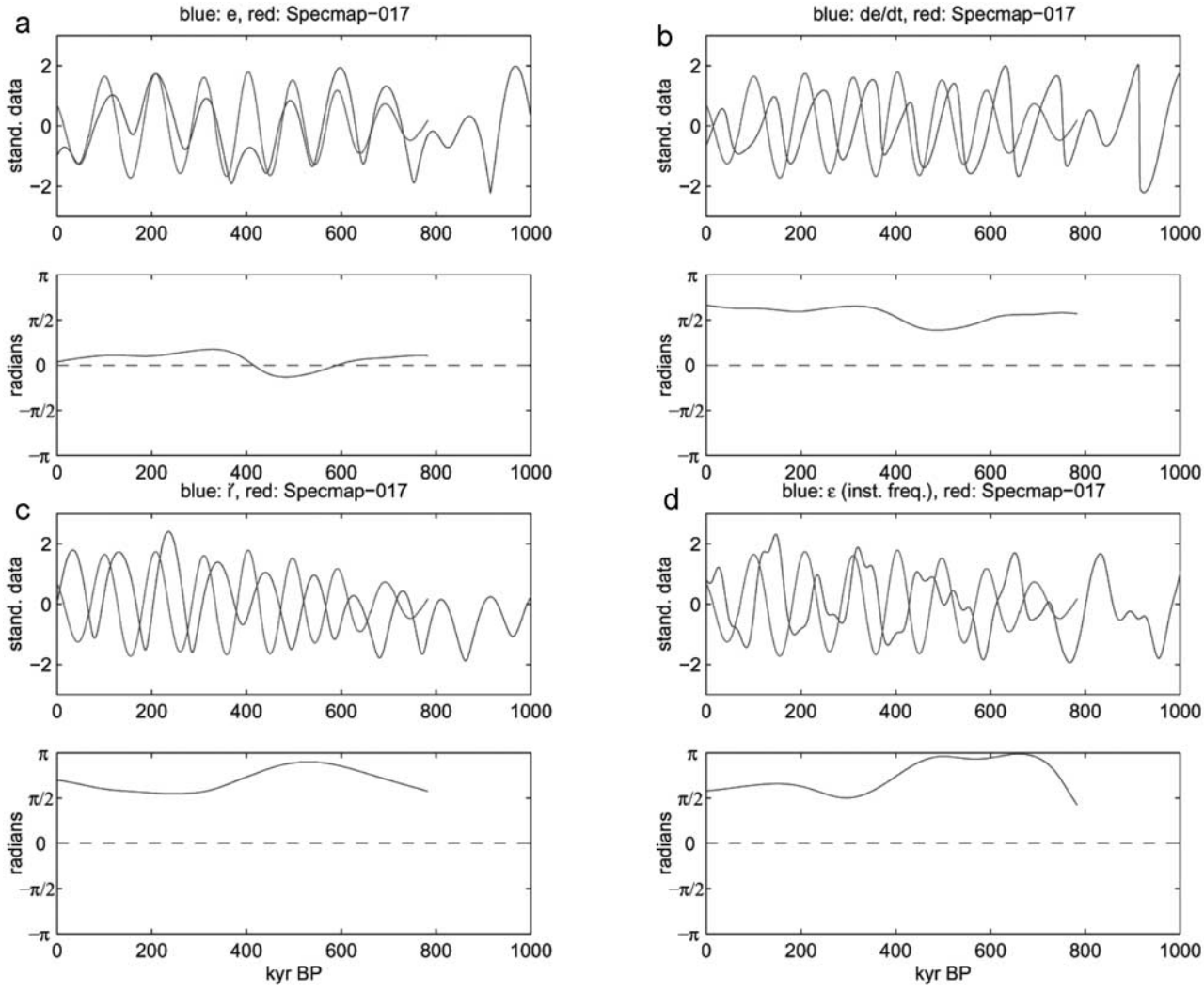

Figure 10. For the SPECMAP geological data shown in Figure 4, a cross-spectrum analysis is made with (a) e, (b) de/dt, (c) i', and (d) instantaneous frequency of ε. In the top panel of Figures 10a–10d the extracted 100-kyr geological signal (red curve) is compared to the astronomical parameter (blue curve), and in the bottom panel the instantaneous phase difference is displayed. See color version of this figure at back of this issue.

with the time series of the four different astronomical parameters described above. For the wavelet transforms where edge effects are present, the estimated amplitudes weaken outside the so-called cone of influence. We corrected these amplitudes by comparing, for all periods, the amplitude of the wavelet transform of these proxy records to the amplitude of the wavelet transform of pure sine waves. The correction applied is inversely proportional to the ratio of the amplitudes.

[27] All data (Figures 4–9) show clearly the progressive strengthening of the 100-kyr signal starting about 700 to 600 kyr B.P., except for Bassinot where it starts at about 800 kyr B.P. There is definitely a gradual change from the 41- to the 100-kyr period with a linearly increasing length of the dominant component in the 100-kyr band: A period slightly less than 95 kyr is dominating in the vicinity of 400 kyr B.P., whereas it becomes between 95 and 123 kyr in the vicinity of 200 kyr B.P. and reaches about 123 kyr for the present.

[28] The next step was to extract the 100-kyr signal from the geological records and compare it with the four different astronomical parameters in order to compute the instantaneous phase difference (for the technique see *Mélice and Servain* [2003]). The best agreement (Figures 10–15) is definitely between e and all the geological records. An almost perfect phase relationship is observed for SPECMAP, Shackleton, and EPICA, although it is the case for Bassinot only up to 600 kyr B.P. and for Lisiecki-Raymo and Tiedemann only up to 700 kyr B.P. For these time series, the data get progressively out of phase for earlier times.

[29] The second best fit is with de/dt which leads the geological records by a constant interval of about 25 kyr in SPECMAP, Shackleton, and EPICA, the same being true

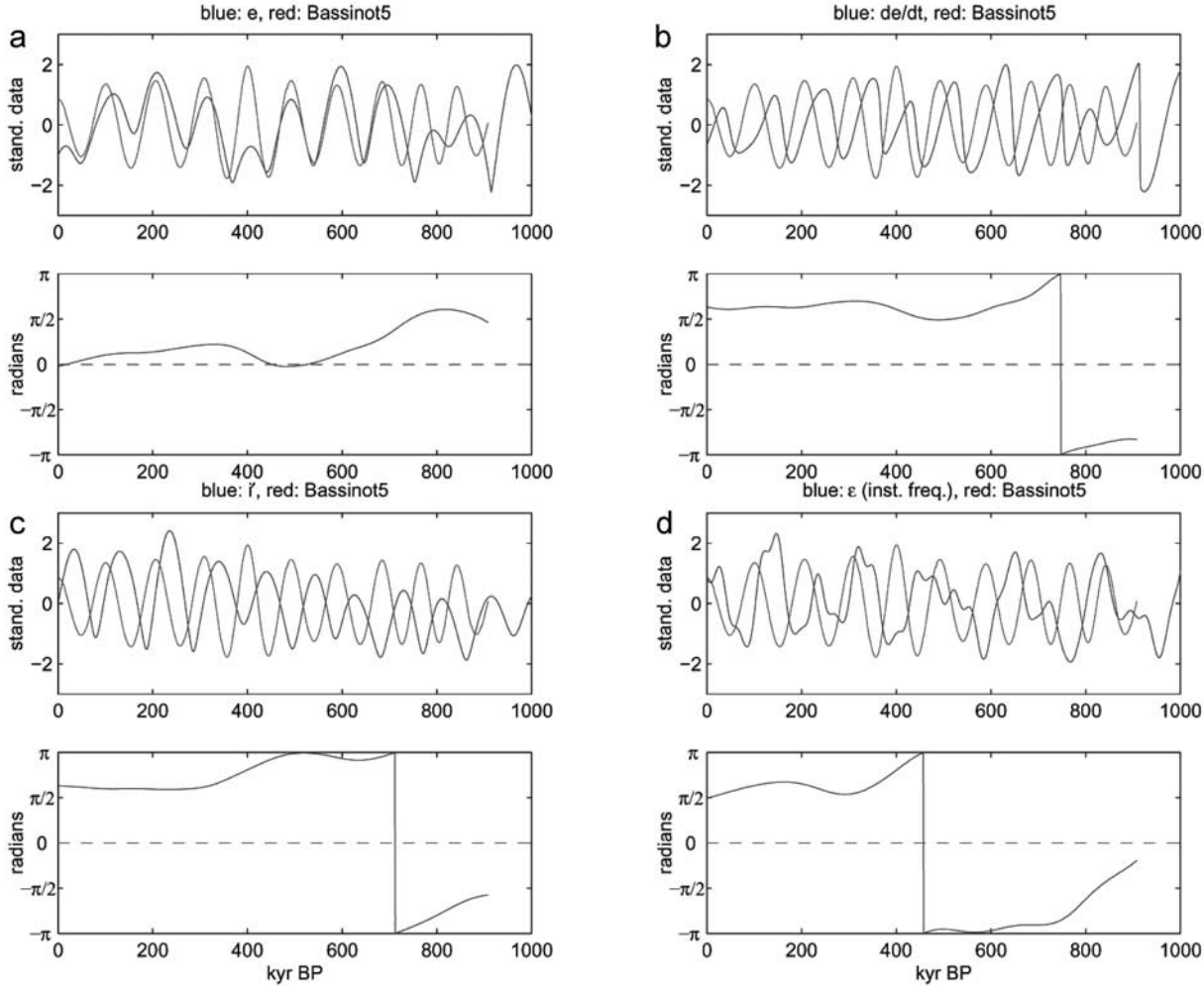

Figure 11. Same as Figure 10 but for the Bassinot data shown in Figure 5. See color version of this figure at back of this issue.

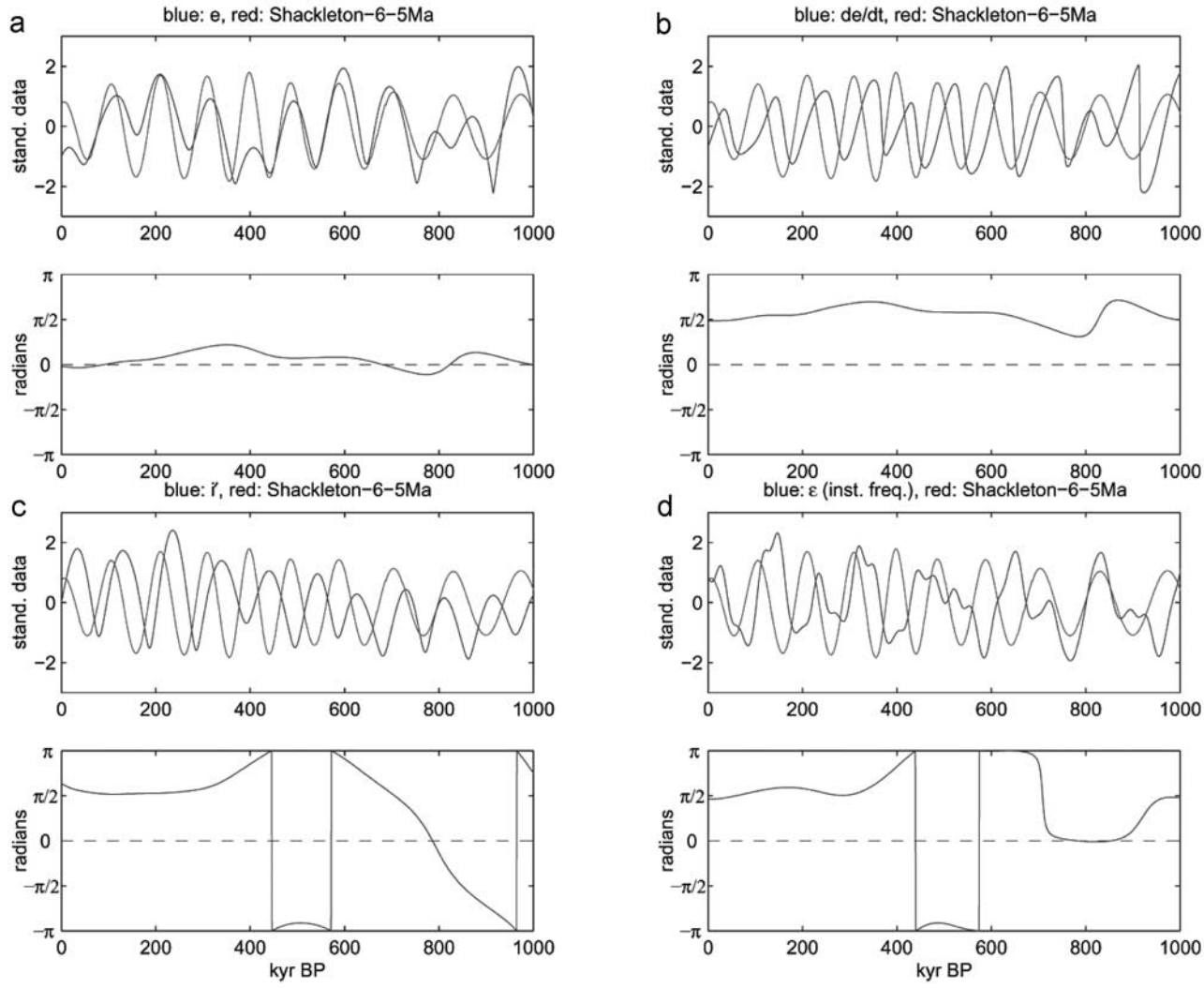

Figure 12. Same as Figure 10 but for the Shackleton data shown in Figure 6. See color version of this figure at back of this issue.

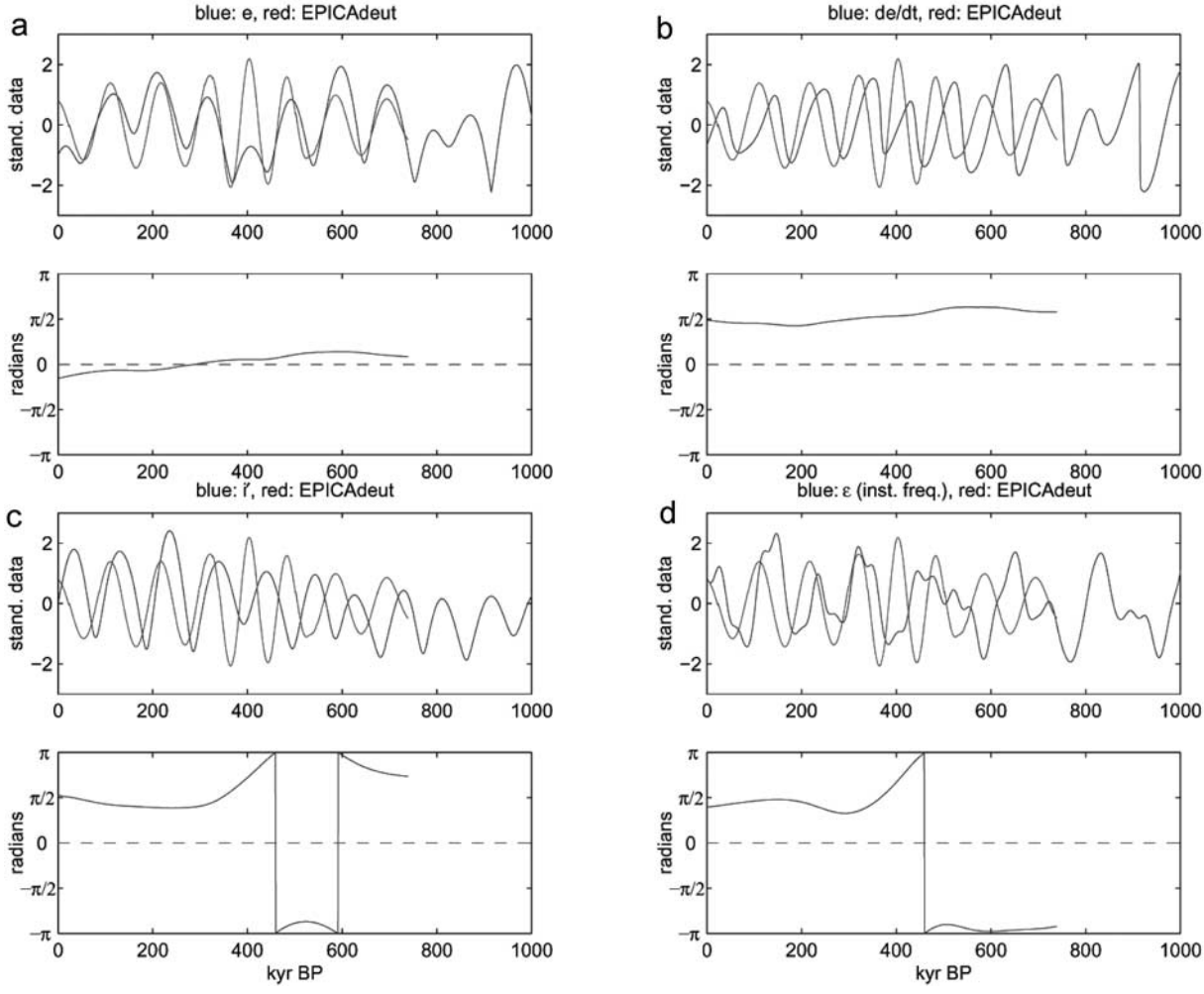

Figure 13. Same as Figure 10 but for the EPICA data shown in Figure 7. See color version of this figure at back of this issue.

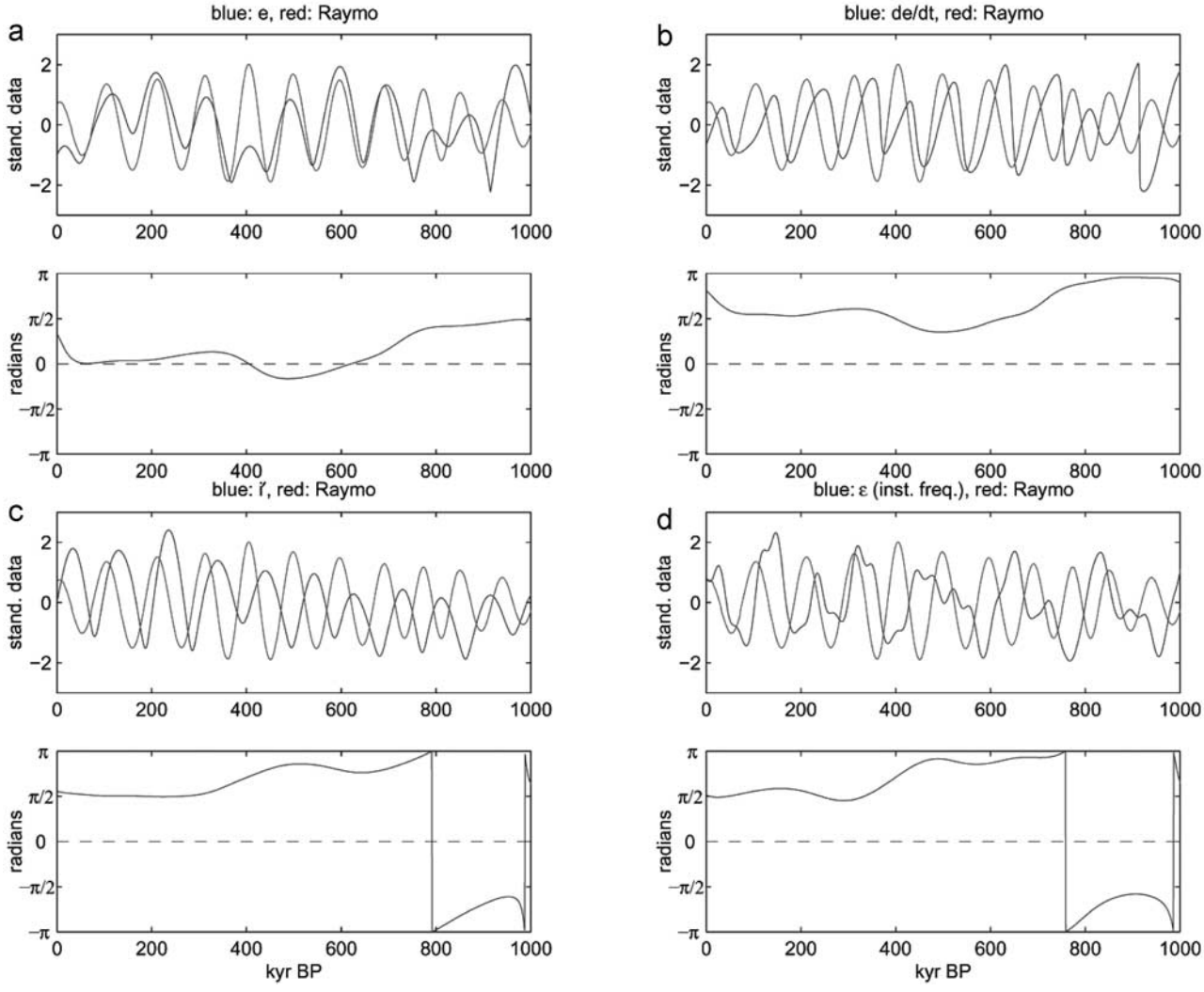

Figure 14. Same as Figure 10 but for the Lisiecki-Raymo data shown in Figure 8. See color version of this figure at back of this issue.

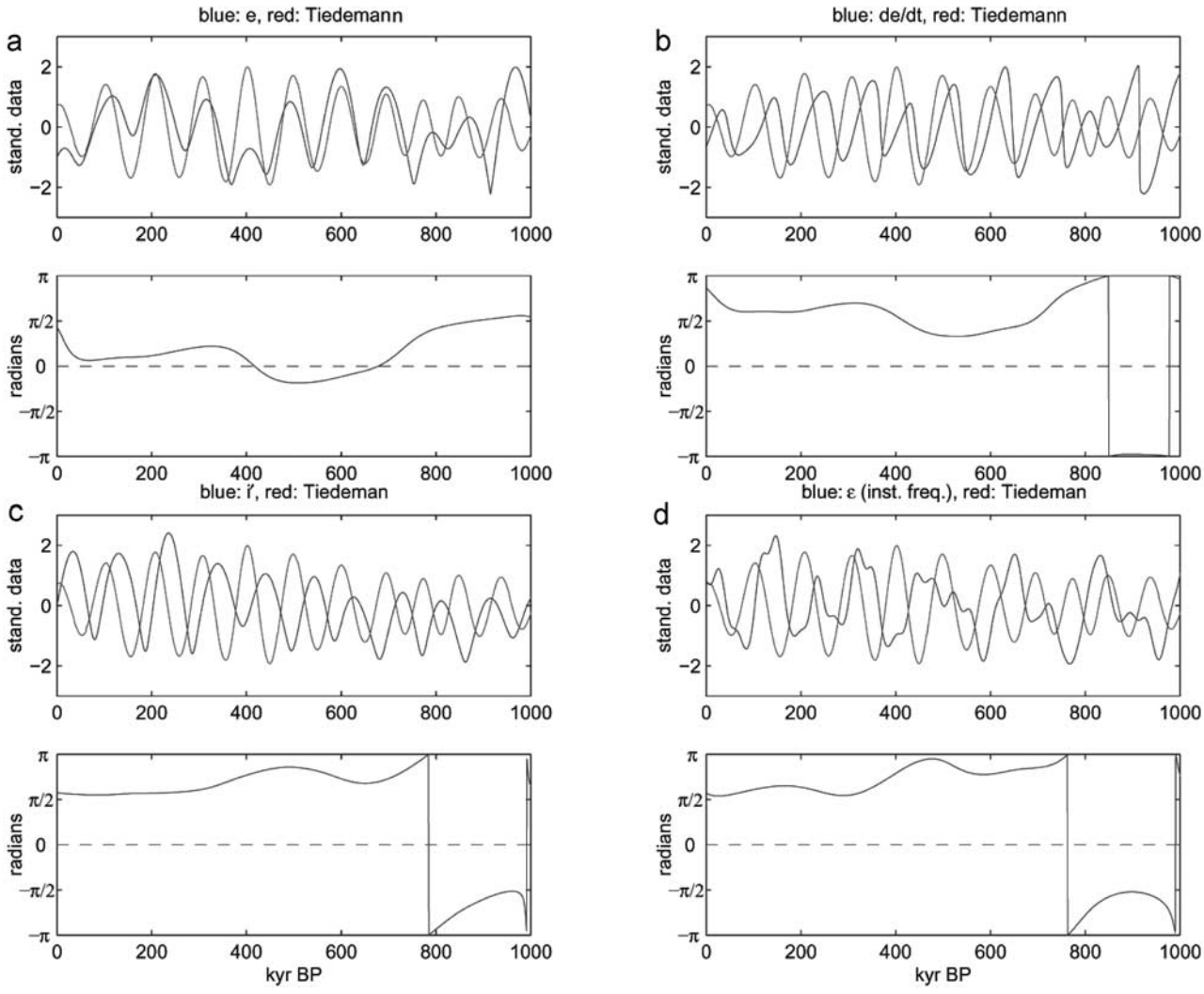

Figure 15. Same as Figure 10 but for the Tiedemann data shown in Figure 9. See color version of this figure at back of this issue.

for the other three geological records except for their older part (as for e the difference in phase moves progressively by one fourth of the period). For the other two astronomical parameters, the phase is far from being stable except maybe over the last 300 kyr where i' and the instantaneous frequency of ε lead the geological records by about 25 kyr. Given such phase instability over time, it is therefore difficult to claim that i' or the frequency modulation of ε play a fundamental role in driving the climate of the last million years.

[30] However, an objective analysis of the impact of the astronomical forcing on the climate system must finally include modeling experiments. Such exercise is illustrated in Figure 16 using the response of the Louvain-la-Neuve climate model to the astronomically driven insolation changes and the Vostok CO_2. The wavelet structure of this response is more complex than the wavelet structure of any of the astronomical parameters analyzed here and much closer to the spectrum of the climate proxy record shown in the bottom panel of Figure 16 and Figure 1 for example. Sensitivity analyses keeping constant either CO_2 [*Berger et al.*, 1998b] or insolation [*Loutre and Berger*, 2000] show that the simulated very strong 100-kyr cycle results mainly from nonlinear processes in the climate system in response to the astronomical forcing. Those are mainly the water vapor-temperature feedback, the albedo-temperature feedback (including snow, ice, and vegetation), the impact of the height of the ice sheets and of their distance to the oceans on their growth, and the lithosphere-cryosphere interactions. Removing one of these processes or more considerably weakens the 100-kyr cycle and can even lead to a response far away from any climate reconstruction.

7. Conclusions

[31] As a conclusion, the analytical calculation of the long-term variations of four astronomical elements (e, de/

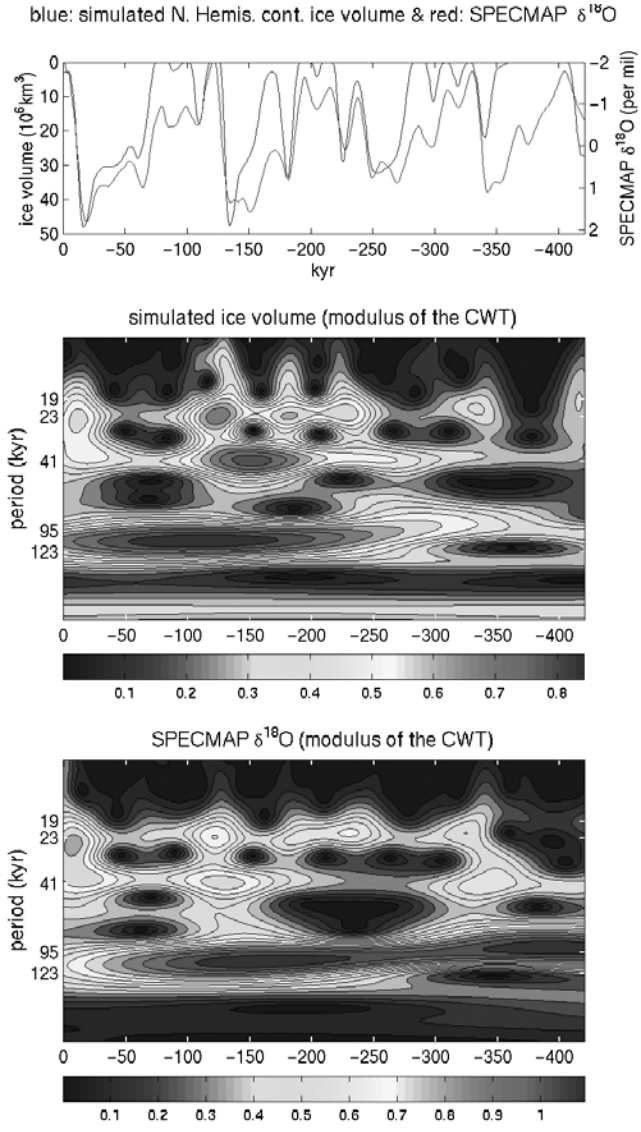

Figure 16. Wavelet analysis of the ice volume simulated by the Louvain-la-Neuve climate model forced by insolation and CO_2 changes [*Berger et al.*, 1998b] and reconstructed by SPECMAP [*Imbrie et al.*, 1984]. See color version of this figure at back of this issue.

dt, i', and frequency modulation of ε) shows that there are actually at least six independent periods approaching 100 kyr in their expansion. Using the *Berger* [1978] solution, these are (1) 94,945 years (from combination tones associated with Mars and Jupiter frequencies) and 99,590 years (coming from Earth-Jupiter interaction), both related to *e*; (2) 98,046 years (Earth and Mercury), 107,478 years (Earth and Venus), and 106,160 years (Mars and Mercury), all three related to i'; and (3) ~97 kyr related to the frequency modulation of ε for which an astronomical origin has not been traced yet. Other periods close to 100 kyr exist but with a much less power; for example, the amplitude associated with 117,308 years in i' is 8 times less than the amplitude of the first term in i'. Some others start to depart more significantly from 100 kyr like 123,297 (Mars-Venus) and 131,248 years (Earth-Venus) which characterize *e* and its derivative. This implies that we must be very cautious in attributing a given signal observed in geological records to a particular astronomical parameter using only such a criteria. Not only these ~100-kyr astronomical periods are close to each others, but their estimated values over a given time interval vary from one sample of time to another. This is actually due to the fact that none of the astronomical parameter is purely periodical, the time-dependent sine waves which constitute the astronomical parameters being responsible for the spectrum changing from one time interval to another (as shown by wavelet analyses). Moreover, these signals can be distorted by the nonlinearity of the response of the climate system to the astronomically forced insolation.

[32] It is therefore recommended that not only the spectra of paleoclimate records be made as accurately as possible, but also that the phase relationship between paleoclimate records and the insolation forcing (or the response of climate models) be analyzed carefully. Finally, the range within which the so-called 100-kyr periods can be found in the astronomical parameters provides an indication of the sampling resolution and accuracy that must be reached in paleoclimate records if it is intended to detect such 100-kyr periodicities in climate reconstructions and attribute them univocally to a given astronomical variable.

[33] Similar conclusions for the last few million years can be drawn qualitatively from more recent astronomical solutions.

[34] **Acknowledgments.** We thank very much F. C. Bassinot, M. E. Raymo, R. Tiedemann, and EPICA for providing their data and J. Imbrie, N. Shackleton, and their collaborators for publishing their data, making them available to the community. The constructive comments of two anonymous reviewers were very much appreciated. We are very grateful to Materne N., who took great care in typing the manuscript.

References

Bassinot, F. C., L. D. Labeyrie, E. Vincent, X. Quidelleur, N. J. Shackleton, and Y. Lancelot (1994), The astronomical theory of climate and the age of the Brunhes-Matuyama magnetic reversal, *Earth Planet. Sci. Lett.*, *126*, 91–108.

Berger, A. (1977), Long-term variations of the Earth's orbital elements, *Celestial Mech.*, *15*, 53–74.

Berger, A. (1978), Long-term variations of daily insolation and Quaternary climatic changes, *J. Atmos. Sci.*, *35*(12), 2362–2367.

Berger, A. (1989), The spectral characteristics of pre-Quaternary climatic records, an example of the relationship between the astronomical theory and geo-sciences, in *Climate and Geo-Sciences*, edited by A. Berger, S. Schneider, and J. C. Duplessy, pp. 44–76, Springer, New York.

Berger, A., and M. F. Loutre (1991), Insolation values for the climate of the last 10 million years, *Quat. Sci. Rev.*, *10*, 297–317.

Berger, A., and M. F. Loutre (1992), Astronomical solutions for paleoclimate studies over the last 3 million years, *Earth Planet. Sci. Lett.*, *111*, 369–382.

Berger, A., and M. F. Loutre (2003), Climate 400,000 years ago, a key to the future?, in *Earth's Climate and Orbital Eccentricity: The Marine Isotope Stage 11 Question*, edited by A. W. Droxler, R. Z. Poore, and L. H. Burckle, *Geophys. Monogr. Ser.*, vol. 137, pp. 17–26, AGU, Washington, D. C.

Berger, A., and M. F. Loutre (2005), Modelling the 100 kyr cycle, an example from LLN EMICS, in *The Climate of Past Interglacials*, edited by F. Sirocko, T. Litt, and M. Claussen, Elsevier, New York, in press.

Berger, A., M. F. Loutre, and C. Tricot (1993), Insolation and Earth's orbital periods, *J. Geophys. Res.*, *98*(D6), 10,341–10,362.

Berger, A., M. F. Loutre, and J. L. Mélice (1998a), Instability of the astronomical periods from 1.5 Myr BP to 0.5 Myr AP, *Palaeoclim. Data Modell.*, *2*(4), 239–280.

Berger, A., M. F. Loutre, and H. Gallée (1998b), Sensitivity of the LLN climate model to the astronomical and CO_2 forcings over the last 200 kyr, *Clim. Dyn.*, *14*(9), 615–629.

Berger, W. H., T. Bickert, H. Schmidt, and G. Wefer (1993), Quaternary oxygen isotope record of pelagic foraminifers: Site 806, Ontong Java plateau, *Proc. Ocean Drill. Program Sci. Results*, *130*, 381–395.

Bretagnon, P. (1974), Termes à longues périodes dans le système solaire, *Astron. Astrophys.*, *30*, 141–154.

Claussen, M., and A. Berger (2005), A survey of hypotheses for the 100 ka cycle, in *The Climate of Past Interglacials*, edited by F. Sirocko, T. Litt, and M. Claussen, Elsevier, New York, in press.

EPICA Community Members (2004), Eight glacial cycles from an Antarctic ice core, *Nature*, *429*, 623–628.

Hays, J. D., J. Imbrie, and N. J. Shackleton (1976), Variations in the Earth's orbit: Pacemaker of the ice ages, *Science*, *194*, 1121–1132.

Imbrie, J., J. Hays, D. G. Martinson, A. McIntyre, A. C. Mix, J. J. Morley, N. G. Pisias, W. L. Prell, and N. J. Shackleton (1984), The orbital theory of Pleistocene climate: Support from a revised chronology of the marine $\delta^{18}O$ record, in *Milankovitch and Climate*, *NATO ASI Ser., Ser. C*, vol. 126, edited by A. Berger et al., pp. 269–305, Springer, New York.

Imbrie, J., et al. (1992), On the structure and origin of major glaciation cycles: 1. Linear responses to Milankovitch forcing, *Paleoceanography*, *7*(6), 701–738.

Imbrie, J., et al. (1993), On the structure and origin of major glaciation cycles: 2. The 100,000-year cycle, *Paleoceanography*, *8*(6), 699–735.

Laskar, J. (1988), Secular evolution of the solar system over 10 million years, *Astron. Astrophys.*, *198*, 341–362.

Laskar, J., F. Joutel, and F. Boudin (1993), Orbital, precessional, and insolation quantities for the Earth from −20 Myr to +10 Myr, *Astron. Astrophys.*, *270*, 522–533.

Lisiecki, L. E., and M. E. Raymo (2005), A Pliocene-Pleistocene stock of 57 globally distributed benthic $\delta^{18}O$ records, *Paleoceanography*, *20*, PA1003, doi:10.1029/2004PA001071.

Liu, H.-S. (1992), Frequency variations of the Earth's obliquity and the 100-kyr ice-age cycles, *Nature*, *358*, 397–399.

Loutre, M. F., and A. Berger (2000), No glacial-interglacial cycle in the ice volume simulated under a constant astronomical forcing and a variable CO_2, *Geophys. Res. Lett.*, *27*(6), 783–786.

Martinson, D. G., N. G. Pisisas, J. D. Hays, J. Imbrie, T. C. Moore Jr., and N. J. Shackleton (1987), Age dating and the orbital theory of the ice ages: Development of a high-resolution 0 to 300,000-year chronostratigraphy, *Quat. Res.*, *27*, 1–29.

Mélice, J. L., and J. Servain (2003), The tropical Atlantic meridional SST gradient index and its relationship with the SOI, NAO and Southern Ocean, *Clim. Dyn.*, *20*, 447–464.

Mélice, J. L., A. Coron, and A. Berger (2001), Amplitude and frequency modulations of the Earth's obliquity for the last million years, *J. Clim.*, *14*(6), 1043–1054.

Milankovitch, M. (1941), Canon of Insolation and the Ice Age Problem (in German), *Math. Natl. Sci.*, vol. 33, *Spec. Publ. 132*, 633 pp., R. Serbian Sci., Belgrade. (English translation by Isr. Program for Sci. Transl., Jerusalem, 1969.)

Muller, R. A., and G. J. MacDonald (1995), Glacial cycles and orbital inclination, *Nature*, *377*, 107–108.

Olsen, P. E., and D. V. Kent (1999), Long-period Milankovitch cycles from the Late Triassic and Early Jurassic of eastern North America and their implications for the calibration of the Early Mesozoic time scale and the long-term behaviour of the planets, in *Astronomical (Milankovitch) Calibration of the Geological Time-Scale*, edited by N. J. Shackleton, I. N. McCave, and G. P. Weedon, *Philos. Trans. R. Soc. London, Ser. A*, *357*(1757), 1761–1786.

Pestiaux, P., and A. Berger (1984), An optimal approach to the spectral characteristics of deep-sea climatic records, in *Milankovitch and Climate*, *NATO ASI Ser., Ser. C*, vol. 126, edited by A. Berger et al., pp. 417–445, Springer, New York.

Petit, J. R., et al. (1999), Climate and atmospheric history of the past 42,0000 years from Vostok ice core, Antarctica, *Nature*, *399*, 429–436.

Pisias, N. G., and T. C. Moore Jr. (1981), The evolution of Pleistocene climate at time series approach, *Earth Planet. Sci. Lett.*, *52*, 450–458.

Prell, W. L. (1982), Oxygen and carbon isotope stratigraphy for the Quaternary of Hole 502B: Evidence for two modes of isotopic variability, *Initial Rep. Deep Sea Drill. Proj.*, *68*, 455–464.

Quinn, T. R., S. Tremaine, and M. Duncan (1991), A three million year integration of the Earth's orbit, *Astron. J.*, *101*(6), 2287–2305.

Rial, J. A. (1995), On the origin of the long-period saw tooth shape of the late Pleistocene paleoclimate records: The first derivative of the Earth's orbital eccentricity, *Geophys. Res. Lett.*, *22*(15), 1997–2000.

Ridgwell, A. J., A. J. Watson, and M. E. Raymo (1999), Is the spectral signature of the 100 kyr glacial cycle consistent with a Milankovitch origin?, *Paleoceanography*, *14*(4), 437–440.

Ruddiman, W. F., N. J. Shackleton, and A. McIntyre (1986), North Atlantic sea-surface temperatures for the last 1.1 million years, in *North Atlantic Palaeoceanography*, edited by C. P. Summerhayes and N. J. Shackleton, *Spec. Publ. Geol. Soc.*, *21*, 155–173.

Shackleton, N. J. (2000), The 100,000-year ice-age cycle identified and found to lag temperature, carbon dioxide, and orbital eccentricity, *Science*, *289*, 1897–1902.

Shackleton, N. J., and N. G. Pisias (1985), Atmospheric carbon dioxide, orbital forcing and climate, in *The Carbon Cycle and Atmospheric CO_2: Natural Variations Archaen to Present*, *Geophys. Monogr. Ser.*, vol. 32, edited by E. T. Sundquist and W. S. Broecker, pp. 303–317, AGU, Washington, D. C.

Shackleton, N. J., A. Berger, and W. R. Peltier (1990), An alternative astronomical calibration of the lower Pleistocene timescale based on ODP site 677, *Trans. R. Soc. Edinburgh Earth Sci.*, *81*, 251–261.

Shackleton, N. J., I. N. McCave, and G. P. Weedon (1999), Astronomical (Milankovitch) calibration of the geological time scale, in *Astronomical (Milankovitch) Calibration of the Geological Time-Scale*, edited by N. J. Shackleton, I. N. McCave, and G. P. Weedon, *Philos. Trans. R. Soc. London, Ser. A*, *357*(1757), 1731–2007.

Tiedemann, R., M. Sarntheim, and N. J. Shackleton (1994), Astronomic timescale for the Pliocene Atlantic ^{18}O and dust flux records of Ocean Drilling Program site 659, *Paleoceanography*, *9*(4), 619–638.

Wigley, T. M. L. (1976), Spectral analysis: Astronomical theory of climatic change, *Nature*, *264*, 629–631.

A. Berger and M. F. Loutre, Institut d'Astronomie et de Géophysique G. Lemaître, Université catholique de Louvain, Chemin du Cyclotron 2, B-1348 Louvain-la-Neuve, Belgium. (berger@astr.ucl.ac.be)

J. L. Mélice, Institut de Recherche pour le Développement/Department of Oceanography, University of Cape Town, Rondebosch 7701, South Africa. (jmelice@ocean.uct.ac.za)

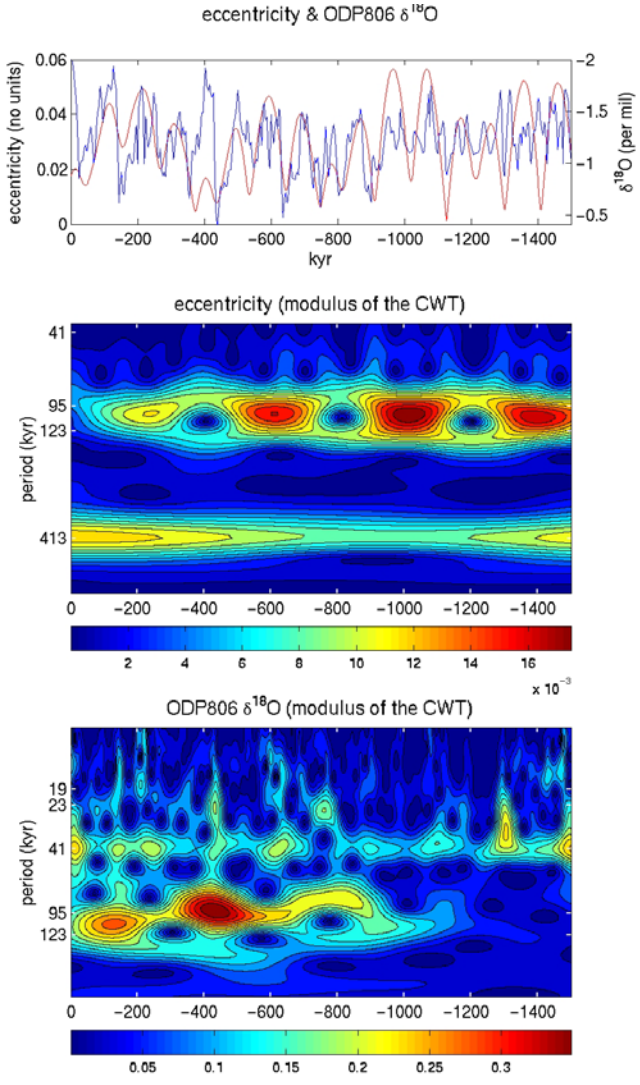

Figure 1. (top) Long-term variations and (middle and bottom) wavelet analysis of eccentricity [*Berger*, 1978] and $\delta^{18}O$ in Ocean Drilling Program (ODP) site 806 [*W. Berger et al.*, 1993].

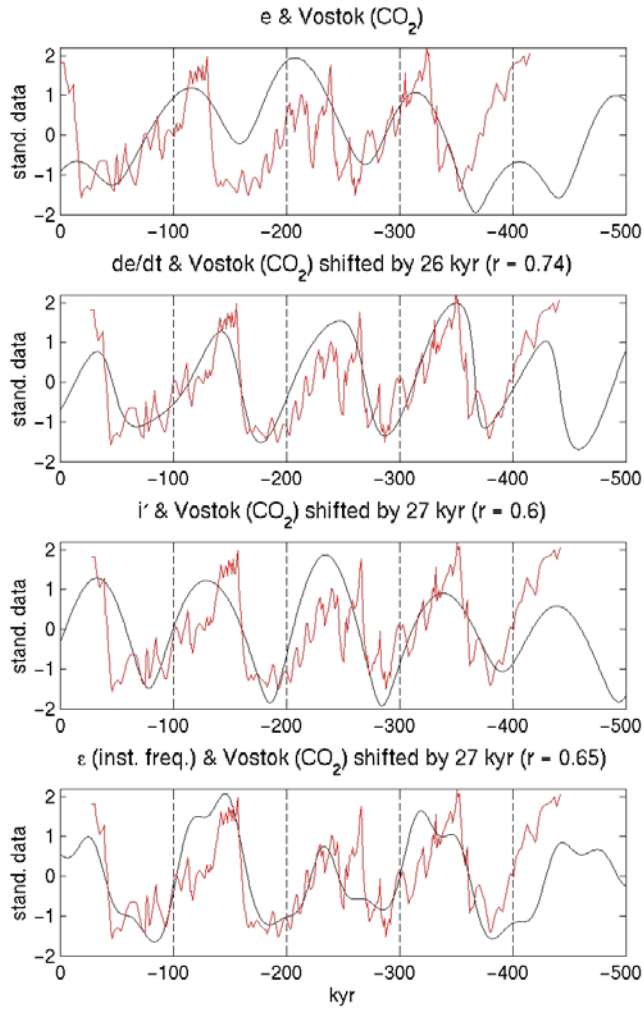

Figure 2. Long-term variations over the last 400 kyr of Vostok CO_2 concentration [*Petit et al.*, 1999], eccentricity, its first derivative, the inclination of the ecliptic on the invariable plane, and the frequency modulation of obliquity using the work of *Berger* [1978]. The time series of the last three parameters have been shifted forward by 26 and 27 kyr.

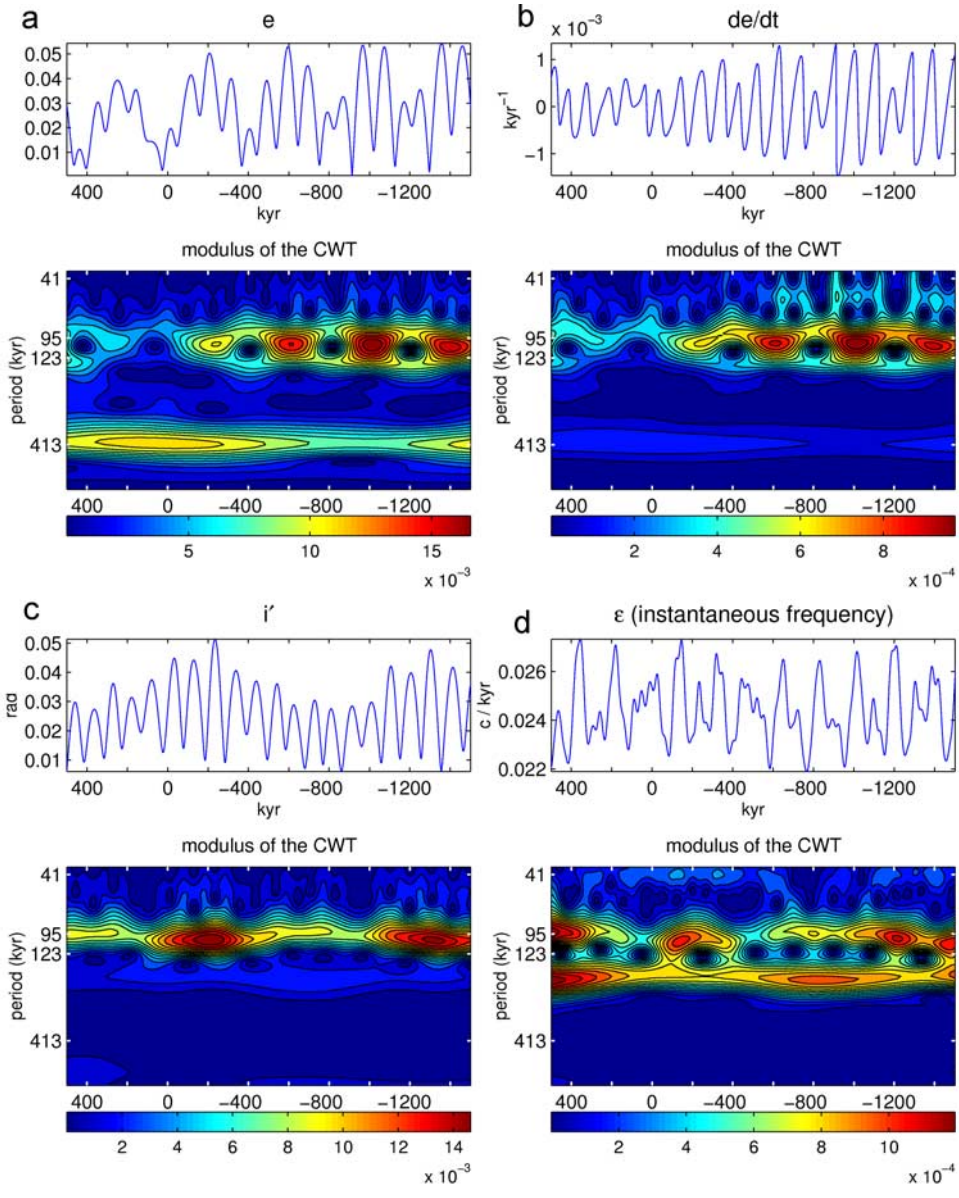

Figure 3. Wavelet analysis of (a) e, (b) de/dt, and (c) i' and (d) of the instantaneous frequency of ε from 1.5 Myr B.P. to 0.5 Myr A.P. (side effects have been eliminated using a much longer interval for the calculation).

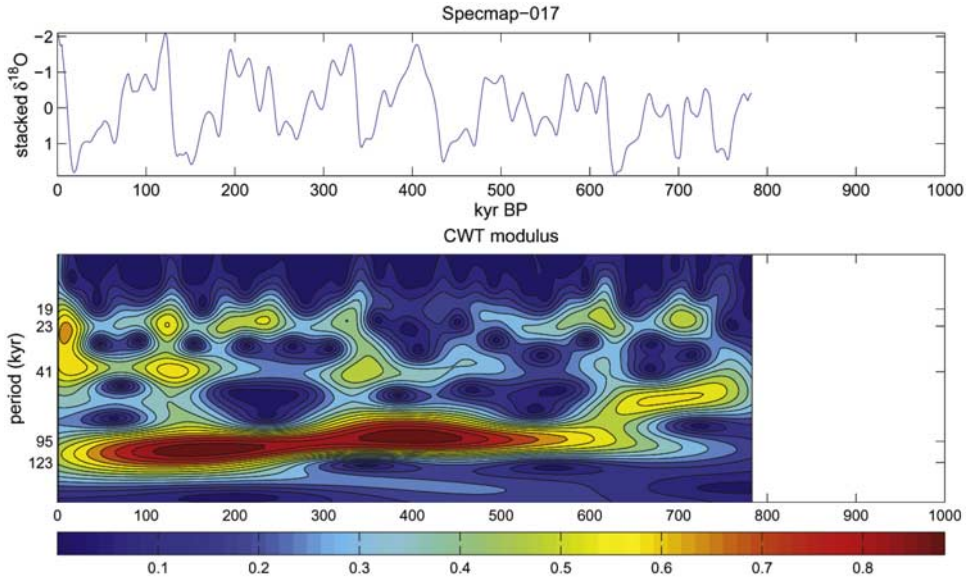

Figure 4. Long-term variations over the last 1 Myr of $\delta^{18}O$ for the (top) spectral mapping (SPECMAP) core and (bottom) a wavelet spectrum. See text for more explanation and references.

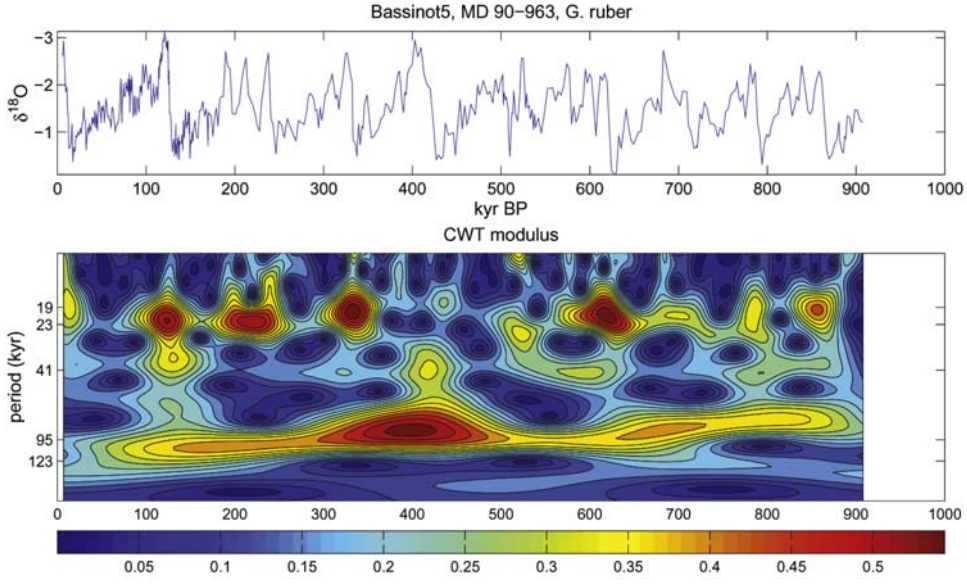

Figure 5. Same as Figure 4 but for the Bassinot core.

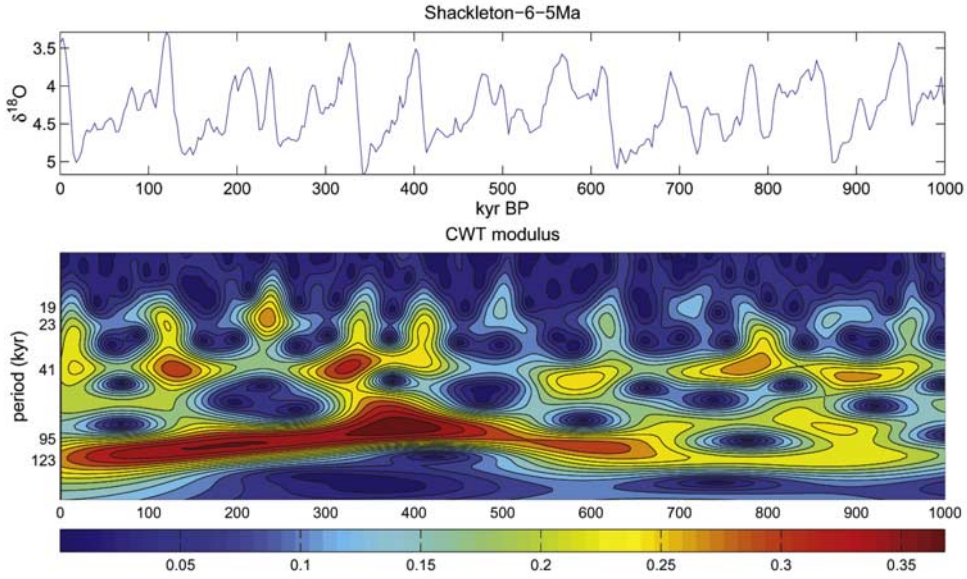

Figure 6. Same as Figure 4 but for the Shackleton core.

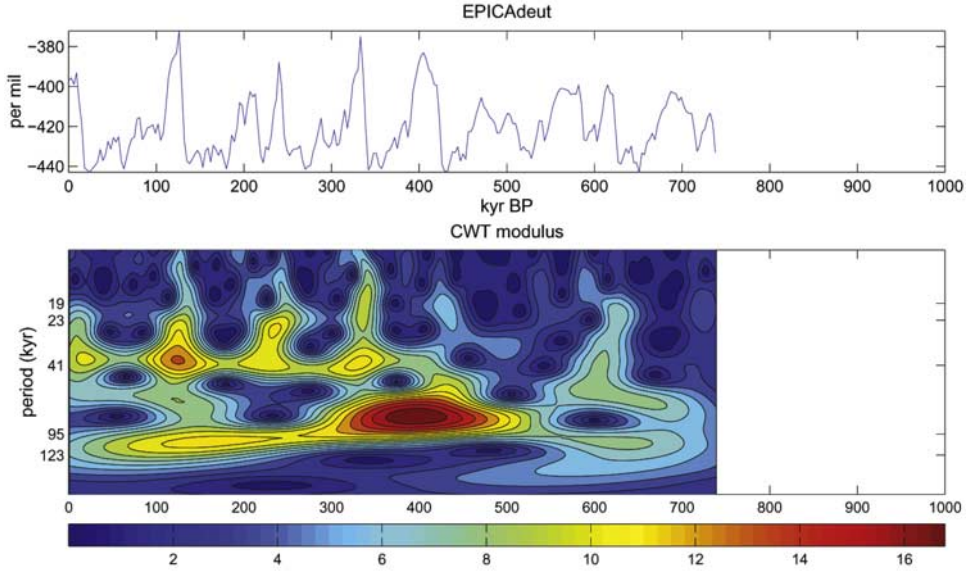

Figure 7. Same as Figure 4 but for the European Programme for Ice Coring in Antarctica (EPICA) deuterium core.

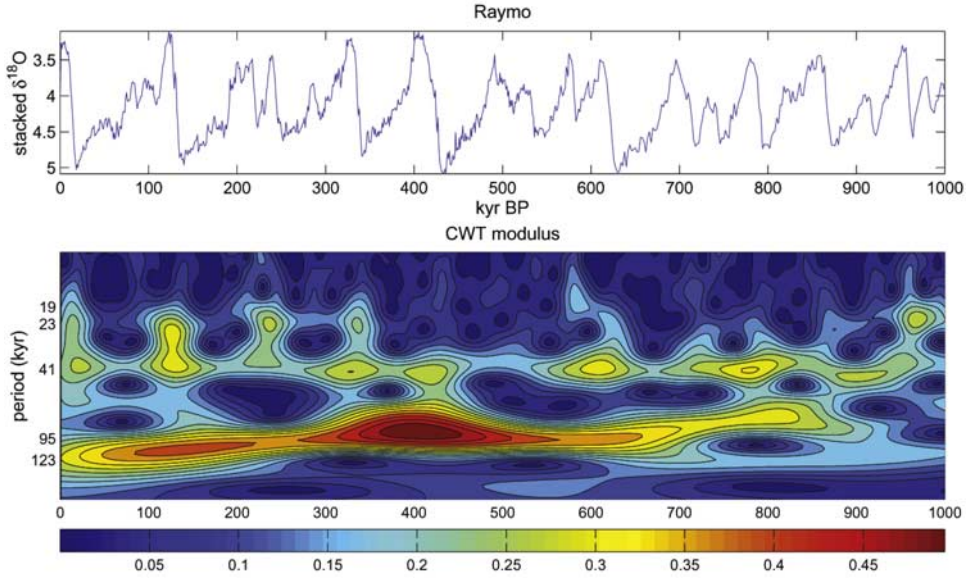

Figure 8. Same as Figure 4 but for the Lisiecki-Raymo core.

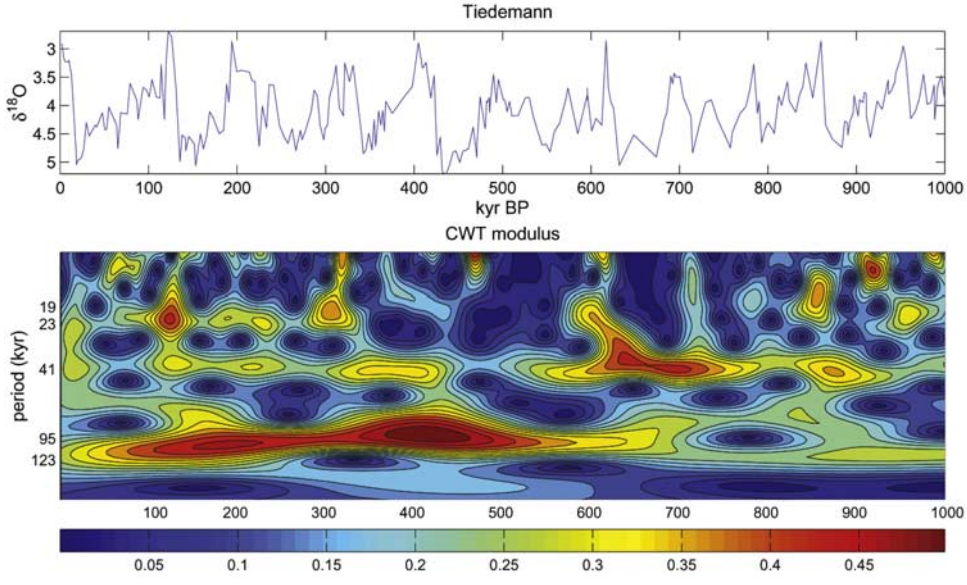

Figure 9. Same as Figure 4 but for the Tiedemann core.

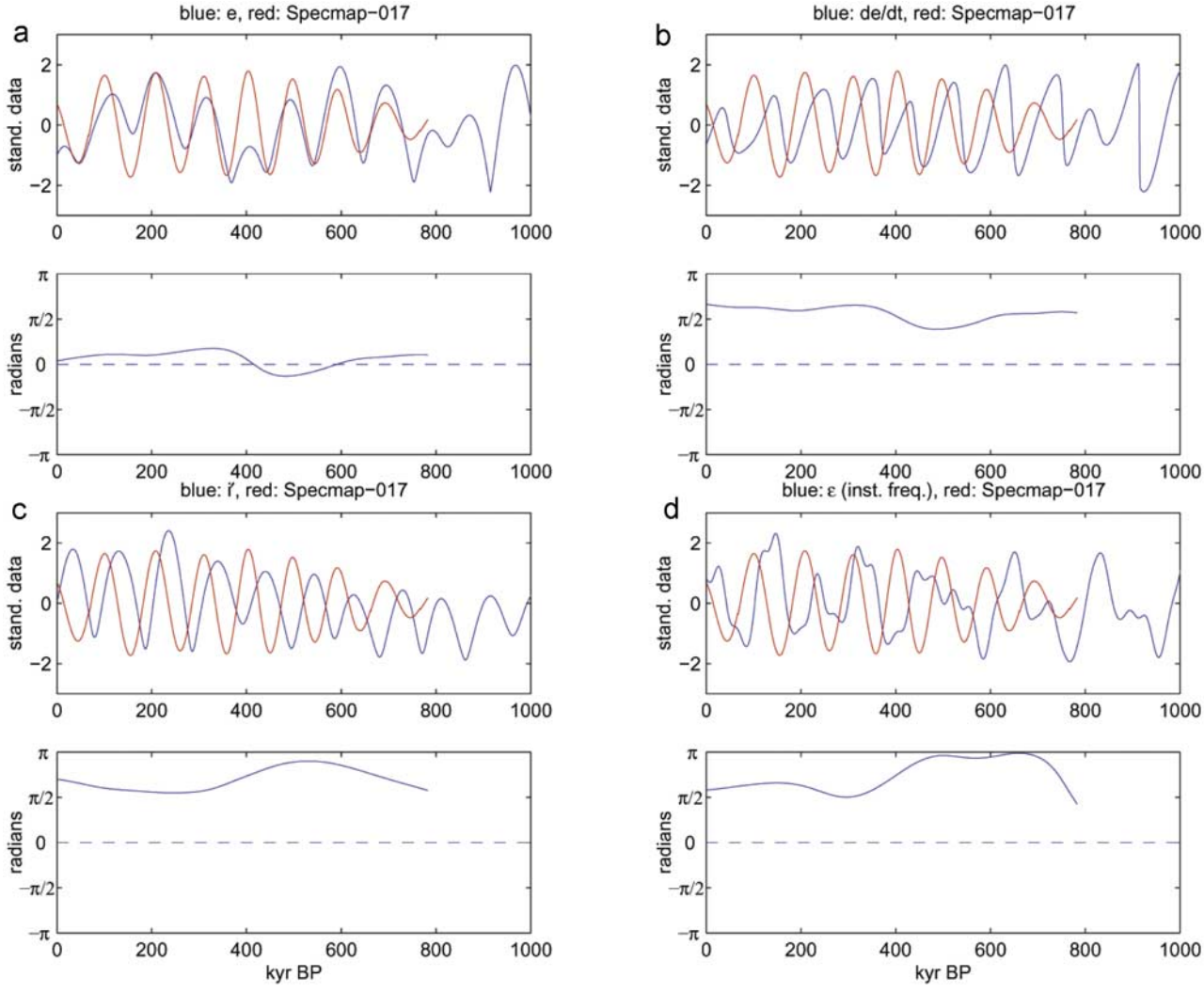

Figure 10. For the SPECMAP geological data shown in Figure 4, a cross-spectrum analysis is made with (a) e, (b) de/dt, (c) i', and (d) instantaneous frequency of ε. In the top panel of Figures 10a–10d the extracted 100-kyr geological signal (red curve) is compared to the astronomical parameter (blue curve), and in the bottom panel the instantaneous phase difference is displayed.

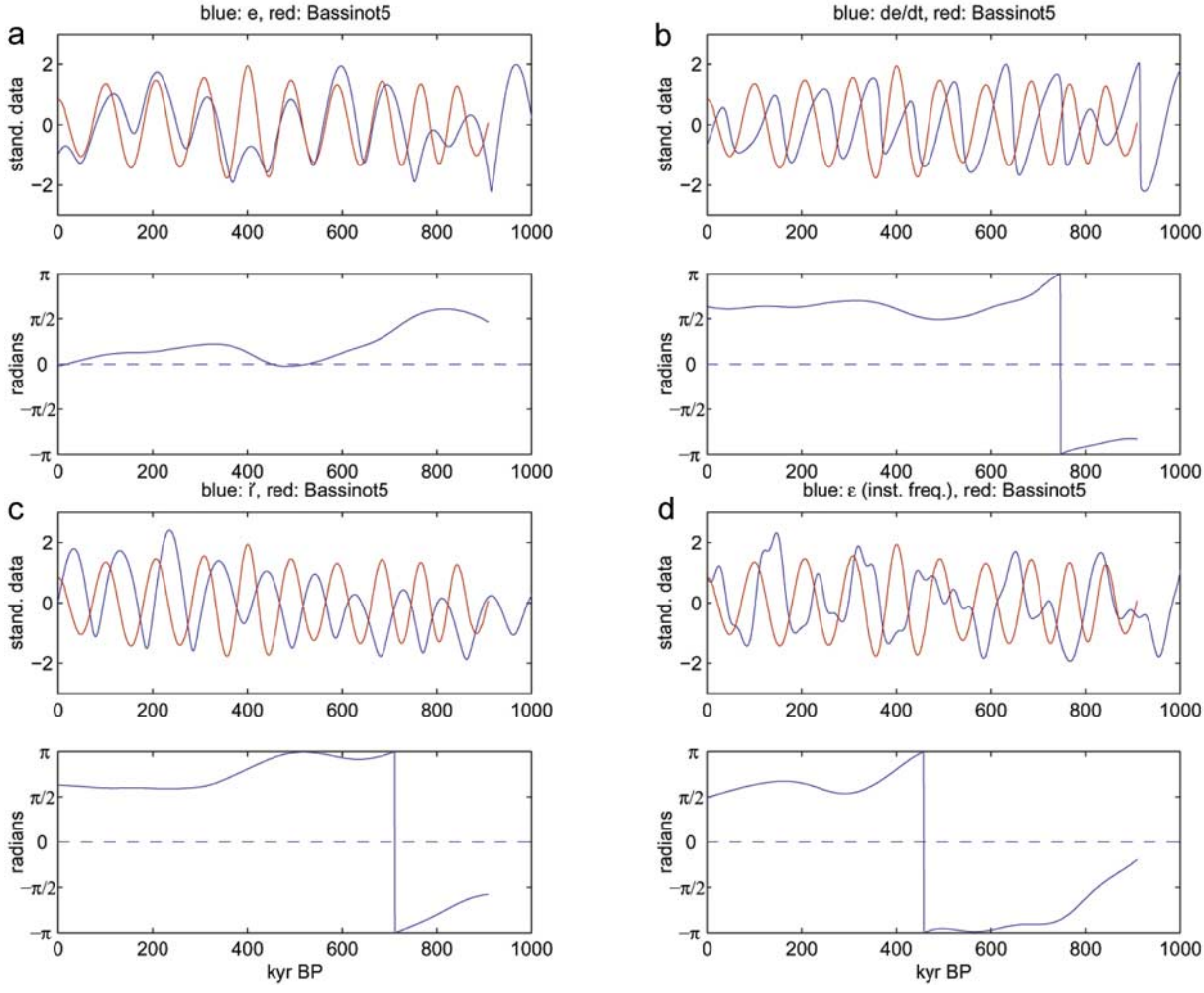

Figure 11. Same as Figure 10 but for the Bassinot data shown in Figure 5.

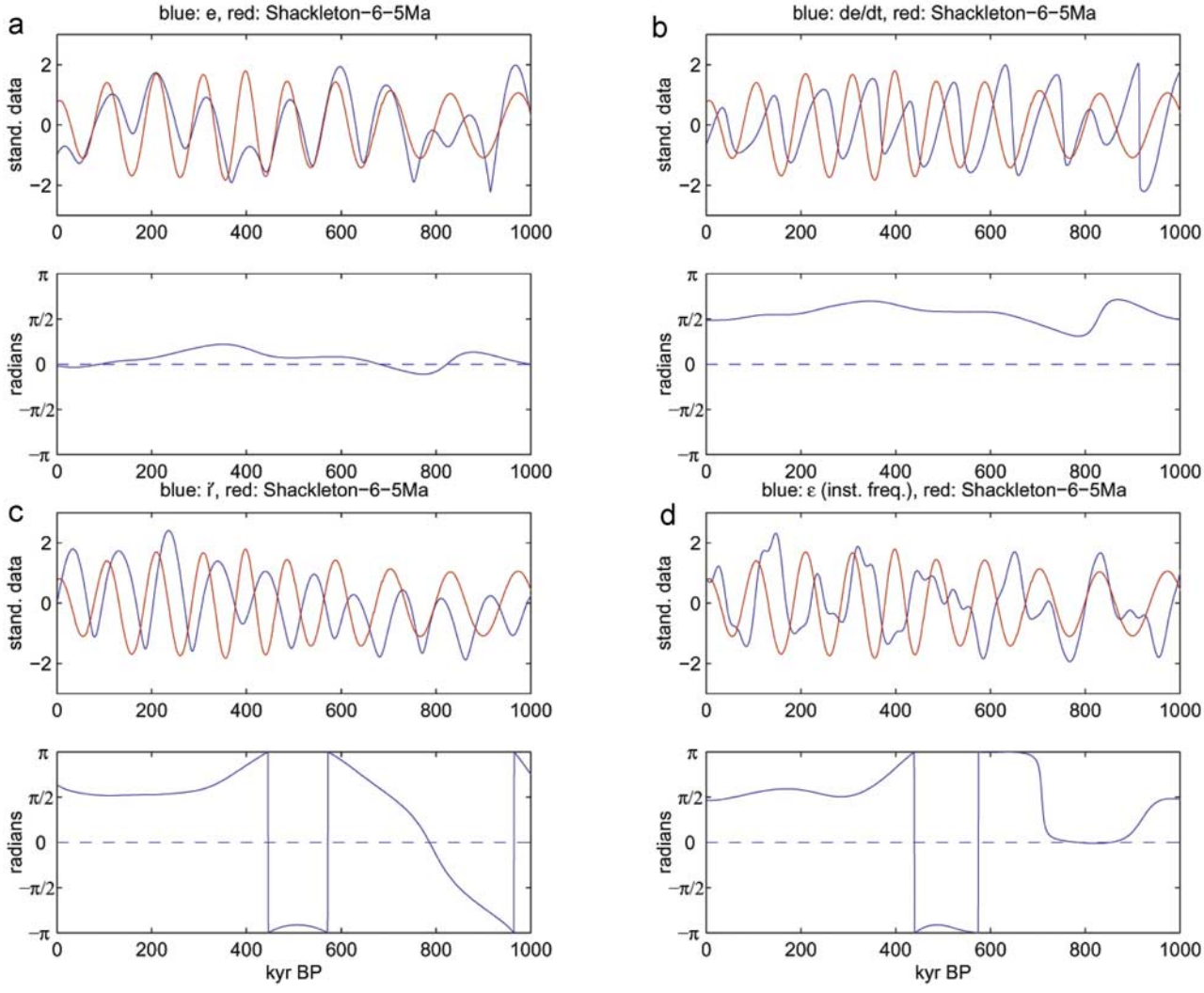

Figure 12. Same as Figure 10 but for the Shackleton data shown in Figure 6.

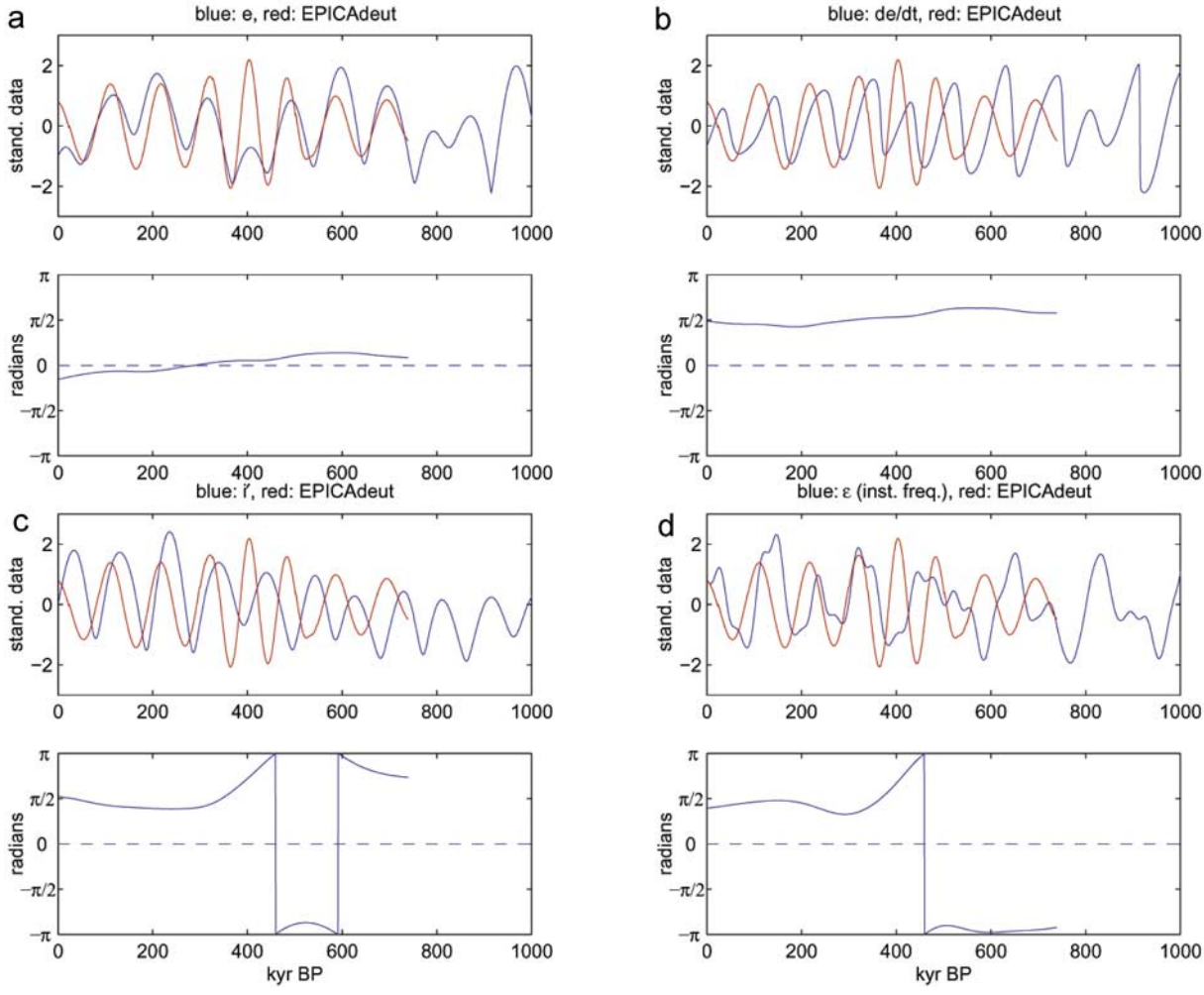

Figure 13. Same as Figure 10 but for the EPICA data shown in Figure 7.

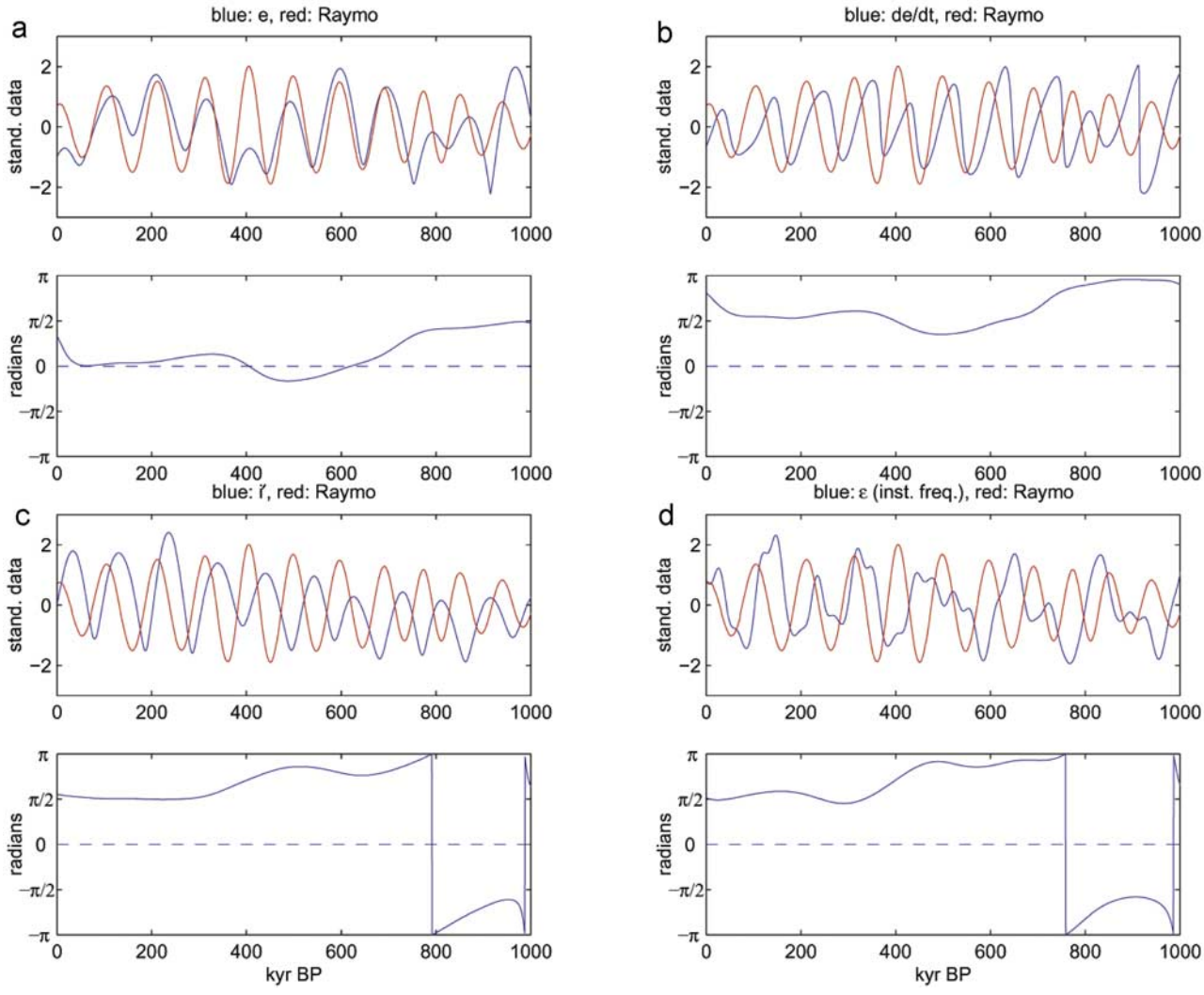

Figure 14. Same as Figure 10 but for the Lisiecki-Raymo data shown in Figure 8.

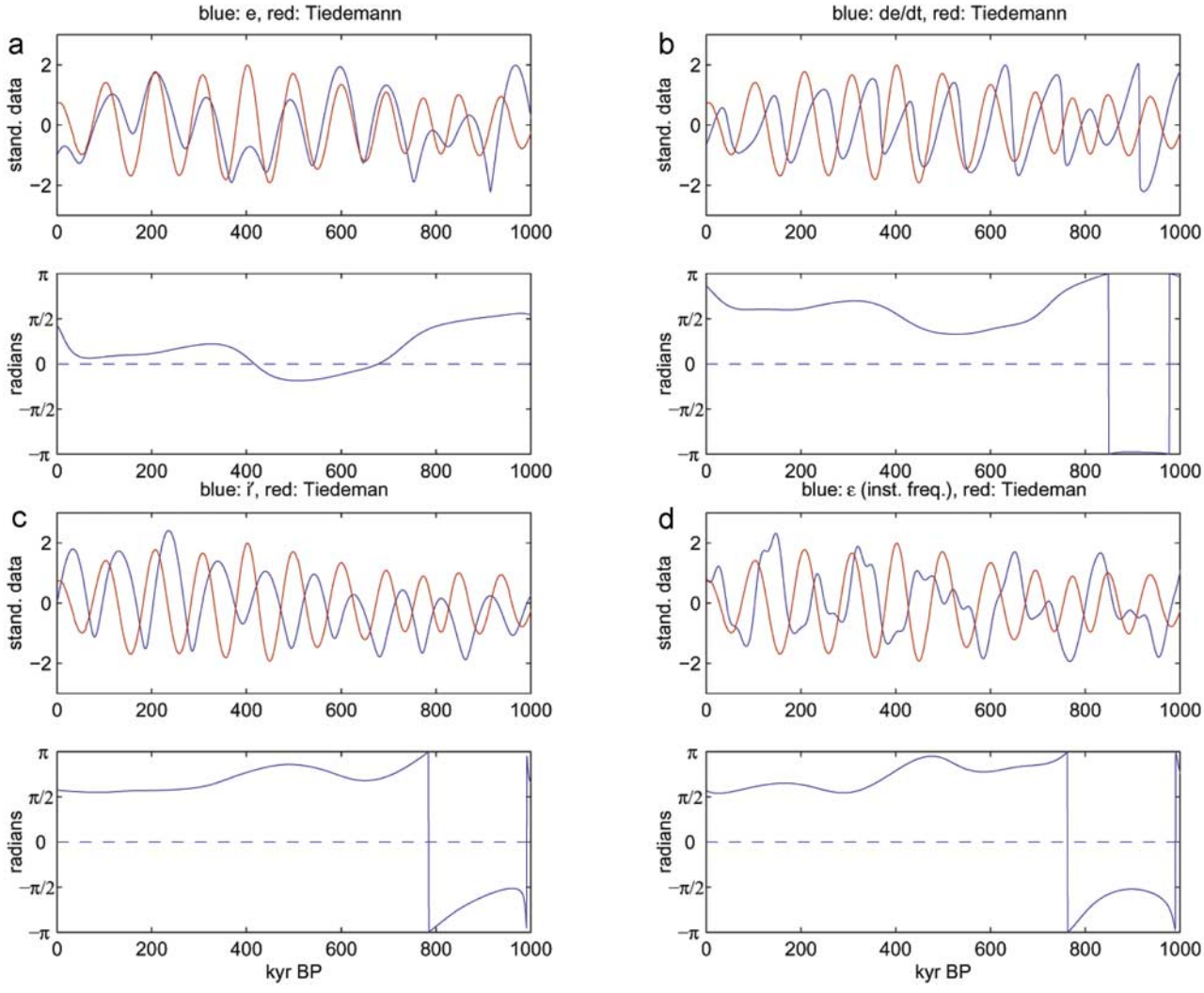

Figure 15. Same as Figure 10 but for the Tiedemann data shown in Figure 9.

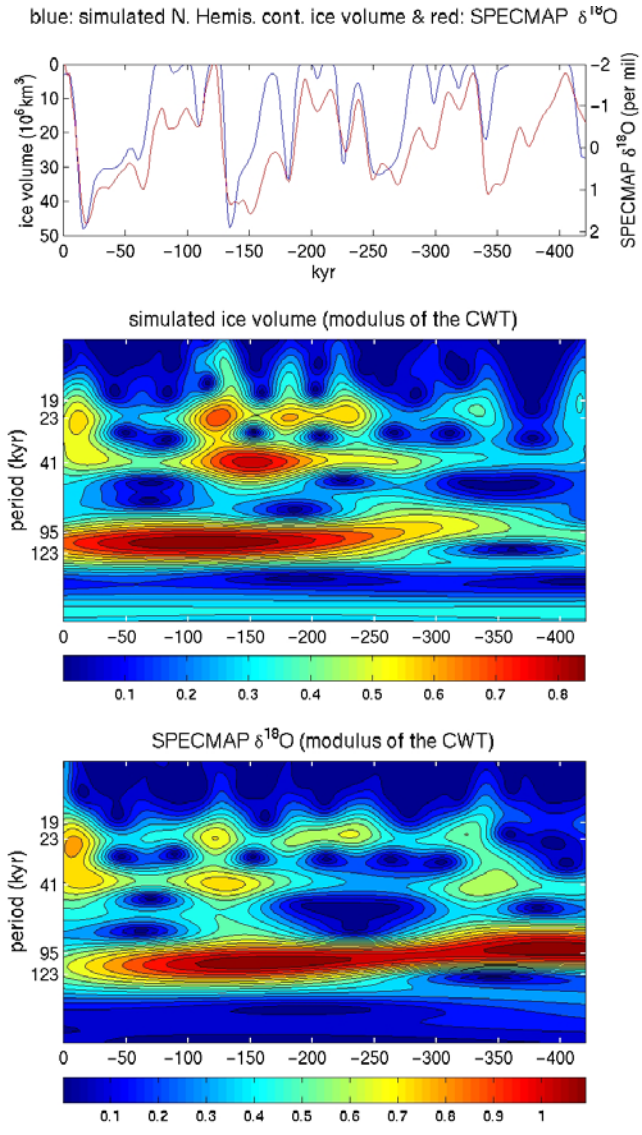

Figure 16. Wavelet analysis of the ice volume simulated by the Louvain-la-Neuve climate model forced by insolation and CO_2 changes [*Berger et al.*, 1998b] and reconstructed by SPECMAP [*Imbrie et al.*, 1984].